Published in final edited form as:

Eur J Med Chem. 2018 December 05; 160: 207–228. doi:10.1016/j.ejmech.2018.10.015.

Novel 5-(quinuclidin-3-ylmethyl)-1,2,4-oxadiazoles to investigate the activation of the α7 nicotinic acetylcholine receptor subtype: Synthesis and electrophysiological evaluation

Marta Quadri[a,b], **Almin Silnović**[a], **Carlo Matera**[a], **Nicole A. Horenstein**[c], **Clare Stokes**[b], **Marco De Amici**[a], **Roger L. Papke**[b], and **Clelia Dallanoce**[a,*]

[a] Department of Pharmaceutical Sciences, Medicinal Chemistry Section "Pietro Pratesi, University of Milan, Via L. Mangiagalli 25, 20133, Milan, Italy

[b] Department of Pharmacology and Therapeutics, University of Florida, P.O. Box 100267, Gainesville, FL, 32610-0267, USA

[c] Department of Chemistry, University of Florida, P.O. Box 117200, Gainesville, FL, 32611-7200, USA

Abstract

α7 nicotinic acetylcholine receptors (nAChRs) are relevant therapeutic targets for a variety of disorders including neurodegeneration, cognitive impairment, and inflammation. Although traditionally identified as an ionotropic receptor, the α7 subtype showed metabotropic-like functions, mainly linked to the modulation of immune responses. In the present work, we investigated the structure-activity relationships in a set of novel α7 ligands incorporating the 5-(quinuclidin-3-ylmethyl)-1,2,4-oxadiazole scaffold, i.e. derivatives **21a**-**34a** and **21b**-**34b**, aiming to identify the structural requirements able to preferentially trigger one of the two activation modes of this receptor subtype. The new compounds were characterized as partial and silent α7 nAChR agonists in electrophysiological assays, which allowed to assess the contribution of the different groups towards the final pharmacological profile. Overall, modifications of the selected structural backbone mainly afforded partial agonists, among them tertiary bases **27a**-**33a**, whereas additional hydrogen-bond acceptor groups in permanently charged ligands, such as **29b** and **31b**, favored a silent desensitizing profile at the α7 nAChR.

Keywords

α7 nicotinic acetylcholine receptor; Electrophysiological studies; Partial agonist; Silent agonist; 1,2,4-Oxadiazoles; Quinuclidine

* Corresponding author. clelia.dallanoce@unimi.it (C. Dallanoce).

Appendix A. Supplementary data

Supplementary data to this article can be found online at https://doi.org/10.1016/j.ejmech.2018.10.015.

1. Introduction

The α7 nicotinic acetylcholine receptor (nAChR) is characterized by low probability of channel opening, rapid concentration-dependent desensitization, and high calcium permeability, which differentiates it from other nicotinic receptor subtypes [1–3]. Besides being widely distributed in the central and peripheral nervous systems, the α7 nAChR is present in non-neuronal cells including immune cells, adipocytes, and intestinal and lung cells [4]. Investigation of this receptor subtype evidenced its crucial roles in neuroprotection [5] and neurogenesis [6], cognitive processes [7], and modulation of inflammatory responses [8,9]. Agonists and partial agonists of the α7 receptor displayed favorable profiles for beneficial treatment of disorders with neurological, neurodegenerative, and neuroinflammatory components [10]. A number of α7 full and partial agonists including GTS-21 (**1**) [11,12], BMS-933043 (**2**) [13], TC-5619 (**3**) [14–16], PNU-282987 (**4**) [17], EVP-6124 (**5**) [18], MEM3454 (**6**) [19], and AR-R17779 (**7**) [20] have moved into clinical trials (Fig. 1A). We designed and tested spiroisoxazoline (*R*)-ICH-3 (**8**) (Fig. 1B), which behaved as a potent and selective α7 agonist and was able to reduce pain and protect nervous tissue in animal models of oxaliplatin-dependent neuropathy. Preclinical eADMET studies and preliminary pharmacokinetic assays indicated the promising drug-like profile of **8** in view of its potential application to CNS disorders [21–23]. Moreover, other scaffolds such as the quinuclidinyl-3(1,2,3-triazole) nucleus (Fig. 1A) provided nicotinic ligands (**9**–**13**) characterized by nanomolar binding affinity for the α7 receptor subtype and promising activity in cognitive impairment models [24–26].

A growing number of literature reports support ionotropic-independent functions of the α7 nAChRs and their involvement in the regulation of inflammatory and immune responses [27]. First evidenced in various non-neuronal cells including microglia and macrophages, these metabotropic-like mechanisms have been further clarified by recent studies on direct coupling of the α7 nAChR subtype to G proteins, both G_{α} and $G_{\beta\gamma}$, through the M3-M4 loop [28–32]. In addition, α7 ligands able to selectively induce nonionotropic activation of the receptor by promoting and stabilizing its desensitized conformations showed interesting anti-inflammatory properties and were proposed as promising therapeutic agents [33–35]. Identified as α7 silent agonists, these compounds show very little partial agonism on their own and favor the positive allosteric modulator (PAM)-sensitive nonconducting D_s state. Indeed, the desensitizing properties of an α7 silent agonist are revealed by co-application of a type II PAM, which evokes channel current activation [36,37]. Different silent compounds (Fig. 1B) such as NS-6740 (**14**) [38], KC-1 (**15**) [36], ASM-024 (**16**) [39], diEPP (**17**) [40], *p*-CF_3-diEPP (**18**) [41], the sulfonium salt **19** [42], and the spirocyclic quinuclidine derivatives **20a** and **20b** [43] were identified, and some of them proved to be effective in *in vivo* anti-inflammatory chronic pain models [44,45]. The study of ligands selective for the α7 receptor evidenced the presence of common pharmacophoric elements in the structures of most full-partial [20,21,25,46–49] as well as silent agonists [36,38–43], including a basic amine, a central group with hydrogen-bond acceptor properties and a lipophilic aryl moiety extending from the amine (Fig. 1A and B).

The possibility of targeting the α7 nAChR by means of dual distinct mechanisms, such as the above mentioned ionotropic and metabotropic-like activation modes, encouraged us to

design new compounds containing the general pharmacophoric features highlighted above. Our goal was to identify novel α7 ligands and focus on the structural requirements able to tune the full, partial, and silent agonist profiles. For the design of the new derivatives we selected the rigid quinuclidine basic nucleus, which is a pivotal moiety in the molecular skeleton of a variety of α7 nAChR ligands [24,50]. Moreover, based on our previous studies on spirocyclic quinuclidinyl-Δ^2-isoxazoline analogs [21,43,48], such as **8**, **20a**, and **20b** which showed full and silent agonism, respectively, we planned to increase the distance between the positive ionizable/ionized quinuclidine ring system and the hydrogen-bond acceptor moiety (Fig. 2). Thus, we explored the insertion of a methylene group between the azabicyclic nucleus and the heterocyclic ring to enhance ligand flexibility and thereby the chance for additional interactions with the receptor protein. Thus, in the new designed derivatives **21a**-**34a** and **21b**-**34b** (Fig. 2), the basic quinuclidine nucleus was connected through a methylene bridge to a 1,2,4-oxadiazole heterocyclic moiety, bearing at the 3-position a *meta*-substituted phenyl or a heterocyclic ring in analogy to the previously studied α7 ligands related to **20a** and **20b**. The *meta*-position of the phenyl ring was probed with different substituents to investigate the α7 binding pocket and tune the electrophysiological activity by favoring additional interactions within the orthosteric recognition domain (Table 1). Substituents were selected to cover a variety of possible connections, spanning from hydrogen bond to halogen bond and π-π interactions.

Herein we describe the synthesis of target compounds as tertiary amines **21a**-**34a** and their corresponding quaternary salts **21b**-**34b** and discuss the changes in the α7 nAChR activation mode following the introduction of different groups on the 5-(quinuclidin-3-ylmethyl)-1,2,4-oxadiazole scaffold.

2. Results and discussion

2.1. Chemistry

The 5-(quinuclidin-3-ylmethyl)-1,2,4-oxadiazole derivatives **21a**-**34a** and **21b**-**34b** were synthesized as racemates according to a one-pot cyclization reaction of a quinuclidine methyl ester intermediate and the appropriate amidoximes under basic conditions [51,52]. The synthetic route for the preparation of the methyl ester derivative **38** is outlined in Scheme 1. Commercially available quinuclidin-3-one **35** was reacted with trimethyl phosphonoacetate in dry tetrahydrofuran and in the presence of sodium hydride [53]. The Wittig reaction afforded in excellent yield the alkene **36** as a 1:1 mixture of the (*E*) and (*Z*) isomers, which was reduced by hydrogenation over palladium on carbon to give intermediate **37**. Subsequent protection of the quinuclidine ring nitrogen atom with a 1.0 M solution of borane-THF complex yielded the 3-acetic acid methyl ester quinuclidine-*N*-borane **38** [21,43].

The amidoximes **47**, **48**, **51** were purchased, while their analogs **39–46**, **49**, **50**, **52** were quantitatively synthesized by refluxing the corresponding nitrile precursors with hydroxylamine in ethanol (Scheme 2), according to a standard literature procedure [52].

Key intermediates **53–65** were prepared by employing the quinuclidine-*N*-borane methyl ester **38** and the suitable amidoximes in the presence of cesium carbonate or sodium hydride

as base (Scheme 3). Cesium carbonate did not require anhydrous conditions and allowed the reaction between methyl ester and amidoxime to proceed smoothly and in high yields affording the 1,2,4-oxadiazole intermediates **53–56**, **58–60**, **43**, **65**, **34** (Method A). Conversely, amidoximes **43**, **47**, **48**, **50** did not react efficiently under these conditions and were therefore treated with sodium hydride in the presence of 3 Å molecular sieves in dry tetrahydrofuran to give the corresponding derivatives **57**, **61**, **62**, **64** (Method B). The borane-protecting group was quantitatively removed by treatment of **53–65** with trifluoroacetic acid in acetone and led to the quinuclidinyl free bases **21–33**. Compound **34** was directly prepared in excellent yield by reacting the unprotected quinuclidine methyl ester **37** with methyl amidoxime **52**. On the other hand, the base-promoted cyclization reaction applied to **37** with the other amidoximes proceeded in poor yields and required tricky purification steps. Finally, the free bases **21–34** were converted into the corresponding fumarates **21a**-**34a** or quaternary methyl ammonium derivatives **21b**-**34b** by treatment with fumaric acid or methyl iodide in methanol, respectively.

2.2. Electrophysiology studies

The new 5-(quinuclidin-3-ylmethyl)-1,2,4-oxadiazoles **21a**-**34a** and **21b**-**34b** were assayed on human α7 nAChRs expressed in *Xenopus laevis* oocytes with two-electrode voltage clamping. To investigate the partial agonism, compounds were initially tested at the standard concentration of 30 μM, and the resulting responses were normalized to the control ACh 60 μM (Table 1). Data were analyzed considering both peak amplitude and net charge of the evoked responses, and the ratios of peak to net charge were used to correlate the tested concentration of 30 μM to the compound EC_{50} (half maximal effective concentration) [54]. Moreover, the newly synthesized derivatives were tested in co-application with 10 μM *N*-(5-Chloro-2,4-dimethoxyphenyl)-*N*′-(5-methyl-3-isoxazolyl)-urea (PNU-120596) to further characterize their activity at the α7 nAChRs (Table 2). Type II PAMs, like PNU-120596 (PNU), are known to modulate compound agonism by interacting at the receptor allosteric binding site and affecting the equilibria of receptor states. Indeed, α7 PAMs induce prolonged receptor activation by increasing receptor opening probability and destabilizing the desensitized PAM-sensitive D_s receptor conformational state. These two mechanisms result in potentiated evoked responses compared to those induced by application of the agonists alone. Destabilization of the D_s receptor state and conversion to the kinetically coupled PAM-dependent conductive state induced by type II PAMs allow identification of the so-called α7 silent agonists [36]. Silent compounds are intrinsically weak α7 agonists able to promote receptor desensitization, which can be revealed by co-application of a type II PAM. The threshold for silent agonism was set to one tenth of the response evoked by 60 μM ACh applied alone. Compounds characterized by net charge responses greater than this value are considered partial agonists. Previous experiments [55] identified 10 μM PNU to yield optimal potentiation of a range of concentrations of ACh-evoked currents over a range of ACh concentrations. Therefore, the target derivatives were tested at 30 μM in coapplication with 10 μM PNU, and the evoked net-charge responses were normalized to receptor responses to 60 μM ACh applied alone. The degree of potentiation achieved in the presence of the PAM is quantified as PNU effectiveness and calculated as the ratio of responses evoked in co-application with PNU to responses evoked by the compound applied alone.

The detailed α7 nAChR activity profiles of the new derivatives applied alone or in co-application with PNU are reported in Tables 1 and 2, respectively. Derivatives **21**–**34** displayed varying degrees of partial and silent agonism, mainly depending on both the nature of the substituents on position 3 of the 1,2,4-oxadiazole ring and the presence or absence of the ammonium group.

2.2.1. Partial agonists—According to the experimental protocol described above, we characterized as partial agonists those compounds inducing net-charge responses greater than 0.1 ACh controls. The majority of the tested derivatives belonging to **a** and **b** series displayed weak to strong partial agonist activation of the α7 nAChR (Table 1, Fig. 3). Compounds of the **a** series showed both higher agonist activity and potency compared to their corresponding methylated analogs of the **b** series as evidenced by their peak-to-net-charge ratios (Table 1). As it can be observed after an initial inspection of the data, the nature of the substituent on the oxadiazole ring deeply affects the resulting responses at the α7 nAChR subtype.

As far as the halogen-containing derivatives **21–24** are considered, although they all behaved as partial agonists, tertiary amines of the **a** series and quaternary ammonium salts of the **b** series showed opposite trends of α7 activation. The increment in halogen size, from fluorine to iodine, promoted a significant reduction of partial agonism in the first series, while keeping potency almost constant. On the other hand, the same modifications resulted in a significant increase of partial agonism and potency in the **b** series, with the permanently positively charged quinuclidine. Interestingly, the trifluoromethyl-substituted analog **25** failed to evoke any α7-mediated response in both series. Generally, the trifluoromethyl group is considered a bioisosteric surrogate of the methyl group. However, in our case, the two groups gave rise to quite different properties of the resulting ligands: while the 3-CF_3-substituted derivatives **25a** and **25b** showed no activation, the *m*-tolyl derivative **26a** displayed partial agonism at the α7 nAChR. Introduction of hydrogen-bonding groups, such as in the 3-OMe-substituted analogs **27a**, **27b** and **28a**, resulted in the partial activation of the receptor subtype under investigation. Both unsubstituted phenyl derivatives **33a** and **33b** displayed partial agonism at the α7 receptor, but they differed in the magnitude of the evoked responses, with the tertiary amine **33a** showing a 5-fold greater receptor activation compared to the ammonium analog **33b**. The effects of a heteroaromatic ring substitution on the 1,2,4-oxadiazole moiety was evaluated by insertion of pyridine, furan, and thiophene (analogs **29–32**). These structural variations caused relevant differences within the two series of compounds. In the **a** series, the heteroaromatic rings evoked partial agonism with a wide range of potencies compared to ACh; on the contrary, the same substitution pattern resulted in no or negligible activation if the methylated quinuclidine salts of the **b** series are taken into account. Finally, replacement of the substituted aromatic ring with an aliphatic moiety, i.e. the two methyl analogs **34a** and **34b,** resulted in a lack of any agonist activation of the α7 subtype, thus suggesting the crucial role of the aromatic ring in that position to gain the wanted receptor activation.

The compounds showing partial agonism in the two sets of nicotinic ligands were further investigated to assess the degree of α7 receptor desensitization induced by their application

at 30 μM (Table 2, Fig. 4). Partial and full agonists of the α7 nAChRs are known to induce rapid desensitization of the receptor, which prevents its further activation upon subsequent application of orthosteric ligands. At least two distinct types of desensitization have been identified and distinguished for their sensitivity (D_s) or insensitivity (D_i) to type II PAMs like PNU-120596 (PNU) [55,56]. In the presence of a suitable allosteric modulator, D_s is converted into an open and conductive state, detectable as an ion flux through the channel. On the other hand, D_i is not affected by PAMs and no current is measured. By co-applying 10 μM PNU, we investigated the ratio of D_s and D_i induced by each compound at the given concentration of 30 μM; partial agonists with low PNU responsiveness emerged as better stabilizers of D_i over D_s. In spite of evoking significant channel activation, some of the studied compounds, i.e. **21a-24a, 27a, 22b-24b**, and **32b,** were unable to desensitize the α7 subtype at 30 μM, with responses in coapplication with the PAM equal or lower than the ACh controls. The poor desensitization (D_s) observed for these derivatives may be ascribed to peculiarities of partial agonist PAM-potentiated responses. Indeed, such responses are often characterized by an inverted U-shaped curve, with large responses over a limited concentration range and sharp decrease in channel opening at lower and higher agonist concentrations [34]. The low channel opening in the presence of a type II PAM indicates D_i to be predominant over D_s, while at the apex of the potentiated response, D_s prevails over D_i. The tested partial agonists displayed short lasting desensitization of the α7 nAChR since post-control ACh was not significantly inhibited after compound application (data not shown).

Derivatives **28a, 31a, 32a,** and **33a** showed similar partial agonist net charge responses (0.401 ± 0.020, 0.575 ± 0.038, 0.508 ± 0.029, and 0.602 ± 0.041, respectively) (Table 1) and for all four compounds the peak-to-net-charge ratio indicated an EC_{50} value lower than 30 μM. Despite all compounds being potentiated by co-application of 10 μM PNU, differences emerged in the magnitude of responses (Table 2), with the furan derivative **31a** displaying a 20-fold higher potentiated response (32.3 ± 12.3) than that shown by compounds **28a** and **33a** (1.6 ± 0.3 and 1.7 ± 0.4) and 6-fold higher than that of the corresponding thiophene isosteric analog **32a** (5.0 ± 1.0). We further investigated these compounds at a lower concentration and tested them at 3 μM on α7 nAChRs alone and co-applied with 10 μM PNU (Fig. 5). At 3 μM, **28a, 31a, 32a** and **33a** retained their partial agonist behavior, with a noticeably decreased response affecting derivative **31a** exclusively (0.15 ± 0.03 at 3 μM *vs* 0.58 ± 0.04 at 30 μM). Indeed, PAM coapplication uncovered the hypothesized inverted U-shaped responses for compounds **28a, 32a,** and **33a** by displaying evoked currents of 4.4 ± 1.5, 13.4 ± 1.8, and 17.4 ± 3.0, respectively. Therefore, application of tested compound at 3 μM resulted in a 3-fold enhancement of potentiated response for **28a** and **32a**, and a 10-fold increase for **33a** compared to the potentiated evoked currents at 30 μM.

Two partial agonist derivatives, **30a** and **31a**, were selected for representative electrophysiological traces to show the effect of PNU co-application at the α7 nAChR and stress the differences in partial agonist responses evoked at this subtype (Fig. 6). The peak-to-net-charge analyses implied an EC_{50} value close to 30 μM for **30a** (peak/net charge = 0.8) and lower than 30 μM for **31a** (peak/net charge = 3.7). The different potencies of the two

compounds are highlighted by the corresponding response shapes, broad and longer for **30a** while sharp and shorter for **31a.**

2.2.2. Silent agonists—Some analogs of the **a** and **b** series showed no activation of the α7 nAChR or induced very weak responses at 30 μM. Various derivatives with poor or no α7 channel activation and the ability to induce receptor desensitization as silent agonists have been reported in the recent literature [34,36,40–43]. To study their behavior as α7 receptor desensitizers, derivatives **21**–**34** were tested in co-application with the type II PAM PNU-120596 (PNU) (Table 2, Fig. 7). Tertiary amines **21a**-**34a** and their corresponding *N*-methyl ammonium salts **21b**-**34b** displayed quite distinct properties at 30 μM. Among the tertiary amines, the 3-methyl substituted analog **34a**, the only derivative characterized by the absence of an aromatic or a heteroaromatic moiety, emerged as the sole α7 silent agonist (30 μM: 0.042 ± 0.008), with a PNU-potentiated net-charge response of 5.1 ± 0.3. On the other hand, quaternary ammonium derivatives of the **b** series provided various compounds with silent activity at 30 μM. Derivatives **26b** and **28b**-**30b** displayed weak potentiated responses in co-application with PNU, with net-charge current lower than 4. Worth noting, the furan derivative **31b** emerged as a stronger α7 desensitizer as revealed by PAM co-application (27.9 ± 15.8).

Analogously to partial agonists, silent ligands are α7 desensitizers and selectively stabilize the D_s and D_i receptor conformational states in different ratios. Depending on the induced ratio of D_s and D_i at a given concentration, each ligand is more or less responsive to PNU application, thus resulting in concentration-response inverted U-shaped curves. To investigate their silent activity over a wider range of concentrations and understand where 30 μM is on the U-shaped PNU responses, compounds **34a, 26b, 28b,** and **31b** were further tested at lower concentrations (3 and 10 μM). The lower concentrations resulted in the lack of potentiated response for **34a,** thus suggesting either preferable stabilization of D_i or a closed state at 3 and 10 μM. On the other hand, the three permanently charged ligands showed a variety of results over the tested concentrations. While behaving as a very weak silent agonist at 3 and 30 μM, the *m*-tolyl derivative **26b** evoked a potentiated response of 10.9 ± 2.8 when co-applied with PNU at 10 μM, thus proving that this concentration is at the apex of the above-mentioned inverted U PAM curve for **26b.** The 4-OMe-phenyl analog **28b** induced comparable weak PNU-potentiated responses at 10 and 30 μM and no potentiation at the lowest 3 μM concentration. We confirmed that the permanently charged furan derivative **31b** is the most potent α7 silent agonist in the whole group of analogs, achieving an optimal concentration for PNU potentiation at 30 μM. Interestingly, the furan motif is also present in the α7 prototypical silent agonist NS-6740 (Fig. 1B) and was associated to hydrogen-bonding acceptor properties within the receptor binding pocket [36]. Our data on compound **31b**, together with those collected on **28b**-**30b**, indicate a suitable hydrogen-bonding moiety as a structural requirement to trigger the α7 nAChR silent activation. Indeed, in the entire set of derivatives, compounds with substituents unable to give a hydrogen-bonding interaction, i.e. halogens or methyl groups, were characterized by higher partial agonist responses and lower receptor desensitization at 30 μM (Table 2).

2.3. Structure-activity relationships

The electrophysiological data from whole-cell two-electrode voltage-clamp recordings allowed us to perform a structure-activity relationship (SAR) for the agonist, either partial or silent, profile of the set of novel 5-(quinuclidin-3-ylmethyl)-1,2,4-oxadiazole analogs **21a-34a** and **21b-34b** under investigation. If the results on spirocyclic quinuclidinyl-Δ^2-isoxazoline derivatives are considered [43], lengthening of the distance between the positive ionized quinuclidinyl group and variation of the hydrogen-bond acceptor heterocyclic moiety (Fig. 2) mostly led to partial agonists at the α7 nAChR while preventing its silent activation. Data on the unsubstituted phenyl derivatives **33a** and **33b** suggested that partial agonism is the default profile at α7 nAChRs for ligands containing the 3-phenyl-5-(quinuclidin-3-ylmethyl)-1,2,4-oxadiazole scaffold, since the majority of the tested compounds behaved as moderate to strong partial agonists. However, the nature of the substituents on the phenyl ring, together with its replacement with heteroaromatic moieties, allowed us to tune the electrophysiological profile towards silent agonism or led to inactive compounds. A detailed analysis of the new derivatives evidenced six silent agonists (**34a, 26b** and **28b-31b**) of the α7 receptor subtype and four compounds (**21b, 25a, 25b** and **34b**) devoid of the ability to activate the receptor.

We compared the agonist net-charge responses for tertiary amines of the **a** series and quaternary ammonium salts of the **b** series (Fig. 8). With the exception of the two pairs **25** and **34**, characterized by the lowest agonist responses, the resulting scatter plot indicated an inverse relationship between the net-charge responses obtained with the two series when the compounds have the same substituent on the oxadiazole ring, thus suggesting that multiple features may concur in determining the magnitude of the α7 agonism.

Halogen-substituted ligands were endowed with moderate partial agonism, with increasing size of the halogen atom inducing opposite trends in the **a** and **b** series. Methyl- and trifluoromethyl-substituted analogs failed to display bioisosterism, since CF_3-containing derivatives **25a** and **25b** were inactive while CH_3-containing ligands **26a** and **26b** behaved as partial and silent agonists, respectively. The presence of a polar methoxy group on the phenyl ring strongly promoted partial agonist activity at the α7 receptor, with the exception of **28b** which showed a good silent agonist profile at the tested (10 and 30 μM) concentrations.

A relevant difference among tertiary amines and their corresponding permanently charged analogs emerged by comparing the data on derivatives which incorporate a heteroaromatic moiety, which gave rise to partial agonism in the **a** subgroup or to the absence of any receptor activation in the **b** subgroup. However, excluding the thiophene analog **32b**, these ligands, i.e. **29b, 30b**, and **31b**, displayed good silent agonist properties, highlighting the relevant role of a further hydrogen-bonding acceptor group, in addition to the 5-(quinuclidin-3-ylmethyl)-1,2,4-oxadiazole scaffold, in triggering receptor desensitization. Therefore, as a general observation and in accordance with previously reported results [43], the presence of a methyl ammonium function is most effective in affording compounds possessing a silent profile at α7 nAChRs. However, the absence of an aromatic substituent on the 5-(quinuclidin-3-ylmethyl)-1,2,4-oxadiazole skeleton coupled with the presence of a

tertiary amine core caused silent activity in compound **34a**. These results are in agreement with previous data known for amine-containing silent agonism pharmacophores [41,43], thus evidencing that a permanent positive charge on the nitrogen nucleus is an important but not essential requirement for α7 silent receptor activation.

Finally, the *m*-trifluoromethyl-phenyl substituted analogs **25a** and **25b**, besides lacking partial agonist activity (0.055 ± 0.008 and 0.035 ± 0.004, respectively, Table 1), did not induce desensitization of the α7 receptor subtype and displayed no potentiation in coapplication with PNU (0.1 ± 0.0 and 0.1 ± 0.0, respectively, Table 2). These results underline the differences of the present set of quinuclidinyl-1,2,4-oxadiazoles compared to the spirocyclic quinuclidinyl-Δ^2-isoxazolines recently reported by our research group, where the *m*-trifluoromethyl-phenyl substituted derivative showed the properties of a silent agonist [43]. We further investigated the quaternary ammonium salt **25 b** at the α7 nAChR co-applied with ACh to assess its antagonist activity (Fig. 9, Panel A). In the presence of the tested compound, ACh showed a residual activity of only 10% at the α7 receptor subtype and the post-control ACh was still significantly inhibited (60% residual activity). Once identified as an antagonist at the α7 nAChR, derivative **25b** was tested at the ganglionic α3β4 nAChR to evaluate its selectivity towards the two nicotinic receptor subtypes (Fig. 9, Panel B). It displayed relevant antagonist activity at the α3β4 receptor as indicated by the inhibition of ACh-evoked channel activation. However, the antagonist component of **25 b** at the α3β4 subtype was brief in duration, as proved by the absence of ACh post-control inhibition. The ACh co-application experiments indicate **25b** as an antagonist of the nAChRs devoid of subtype specificity.

3. Conclusion

Selective activation of the α7 nAChR subtype is a therapeutic option for a variety of disorders including cognitive impairment, neurodegeneration, and inflammation. A dual mechanism of activation, involving either the classic ionotropic channel opening or an alternative metabotropic signaling pathway, has been reported for this receptor subtype. Among the ligands that mediate ion channel activation, partial agonists retain robust efficacy in preclinical models over a wider dose-exposure range than agents with a high level of intrinsic efficacy. Besides, silent agonists, which promote α7 receptor desensitization over activation by inducing non-conducting ligand-bound conformational states, appeared to be therapeutically favorable for peripheral pain and inflammatory diseases. Therefore, compounds characterized by a partial or silent agonist profile at the α7 nAChR may represent better drug candidates for α7-related disorders.

In the present study, we aimed at selecting a specific modulation of signal transduction of α7 nAChRs between a dependent and an independent channel activation pathway. To such an end, we planned suitable chemical modifications on the 5-(quinuclidin-3-ylmethyl)-1,2,4-oxadiazole core skeleton, then synthesized and tested the two series of structurally related ligands **21a**-**34a** and **21b**-**34b**. Overall, the set of novel derivatives showed a pharmacological profile which differs from that of the previously investigated quinuclidinyl-Δ^2-isoxazoline spirocyclic compounds [21,43]. As a general trend, in the new group of nicotinic ligands, increasing both ligand flexibility and distance between the cationic center

and the functionalized heterocyclic ring shifted the activity profile towards partial agonism, whereas the more constrained spirocyclic quinuclidinyl-Δ^2-isoxazolines preferentially induced the α7 desensitized PAM-sensitive D_s state.

However, some of the investigated derivatives (**34a**, **26b**, and **28b**-**31b**) displayed a silent agonist profile at the target nicotinic receptor subtype. In agreement with previous data available for the silent α7 derivative NS-6740 (**14**), we found that an additional hydrogen-bond acceptor group within the binding pocket favors the silent desensitizing profile at the α7 nAChR, such as in ligands **28b**, **29b**, **30b**, and **31b**, incorporating a 4-OMe-phenyl ring, a 3- or 4- substituted pyridine, and a furan ring, respectively. Conversely, derivatives bearing groups in the same position unable to give hydrogen-bonding interactions, i.e. halogen and methyl in both **a** and **b** series, did not induce receptor PAM-sensitive desensitization.

4. Experimental section

4.1. Chemistry

All reagents and solvents were purchased from Sigma-Aldrich Srl (Milan, Italy) and were used without further purification. All reactions were carried out under inert atmosphere of argon or nitrogen and monitored by thin-layer chromatography (TLC) on commercial aluminum plates precoated with silica gel 60 (F-254, Merck) or with aluminum oxide (F-254, Fluka). Visualization was performed with UV light at 254 nm. Spots were further evidenced by spraying with a dilute alkaline potassium permanganate solution or a phosphomolybdic acid solution and, for tertiary amines, with the Dragendorff reagent. Glassware was oven-dried or flame-dried prior to use. The synthesized compounds were purified on glass flash chromatography columns packed with silica gel (230–400 mesh particle size, pore size 60 Å, Merck). Melting points of solid products were measured in capillary tubes with a model B 540 Büchi apparatus and are uncorrected. ^{1}H NMR and ^{13}C NMR spectra were recorded with a Varian Mercury 300 (^{1}H, 300.063; ^{13}C, 75.451 MHz) spectrometer at 20°C. Abbreviations used for peak multiplicities are given as follows: s (singlet), bs (broad singlet), d (doublet), t (triplet), q (quartet), m (multiplet). Coupling constants (J) are given in Hz, chemical shifts (δ) are expressed in parts per million (ppm) and calibrated for ^{1}H using TMS and for ^{13}C using residual deuterated solvent as internal standard ($CDCl_3$, 77.16 ppm; CD_3OD, 49.00 ppm; DMSO-d_6, 39.52 ppm). ESI mass spectra were obtained on a Varian 320 LC-MS/MS instrument. Data are reported as mass-to-charge ratio (m/z) of the corresponding positively charged molecular ions. The purity of final compounds was determined using an Agilent Technologies 1200 series HPLC instrument. The HPLC analyses were performed using two different methods: method 1 for tertiary amines **21a-34a** and method 2 for quaternary ammonium salts **21b-34b**. Method 1: Analysis was performed on a LiChroCART 250–4 LiChrosher 100 RP-18 analytical column (5 μm) operating at 25 °C. The injection volume of the sample was 10 μL. Elution was carried out with 3 μM ammonium formate buffer containing 0.1% formic acid as mobile phase A and methanol as mobile phase B (A/B 10:90) at a flow rate of 1 mL/min. Method 2: Analysis was performed on a Supelco Supelcosil LC-SCX analytical column (3 × 250 mm, 5 μm) operating at 40 °C. The injection volume of the sample was 10 μL. Elution was carried out with 50 μM monobasic potassium phosphate buffer (pH = 3) containing 20 μM potassium

chloride as mobile phase A and acetonitrile as mobile phase B (A/B 60:40) at a flow rate of 1 mL/min. All final compounds tested for biological activity showed >95% purity (detection by UV absorption at 207 nm).

4.1.1. 2-(1-Azabicyclo[2.2.2]oct-3-ylidene)-acetic acid methyl ester (36)—A stirred solution of trimethyl phosphonoacetate (7.74 mL, 48.0 mmol, 1.2 equiv) in dry tetrahydrofuran (750 mL) under an argon atmosphere at 0 °C was treated portionwise with sodium hydride 60% dispersion in mineral oil (1.92 g, 48.0 mmol, 1.2 equiv). After stirring for 1 h at room temperature (rt), quinuclidin-3-one **35** (5.00 g, 40.0 mmol, 1 equiv) was added dropwise via a syringe to the mixture and stirring was continued overnight at rt. The reaction completion was confirmed by TLC (dichloromethane/methanol 9:1) and the mixture was cooled to 0 °C and quenched with deionized water (100 mL). The aqueous layer was extracted with dichloromethane (3 × 300 mL) and the organic layers were collected and treated with 1 N HCl (500 mL). The acidic aqueous phase was separated and basified to pH = 9 by portionwise addition of potassium carbonate at 0 °C and then extracted with dichloromethane (3 × 300 mL). The pooled organic phases were dried over anhydrous Na_2SO_4, filtered and concentrated *in vacuo* to obtain compound **36** as a 1:1 mixture of *(E)* and (*Z*) stereoisomers, which was used without further purification in the next reaction step. Yellow, very viscous oil; yield: 7.25 g, 100%; R_f = 0.40 (dichloromethane/methanol 9:1). ^{1}H NMR (300 MHz, $CDCl_3$) δ (ppm): 5.63 (t, J = 2.5Hz, 1H), 5.61 (t, J = 1.7Hz, 1H), 3.94–3.85 (m, 3H), 3.66 (s, 3H), 3.65 (s, 3H), 3.47–3.41 (m, 2H), 2.98–2.71 (m, 8H), 2.48–2.38 (m, 1H), 1.84–1.56 (m, 8H). ^{13}C NMR (75 MHz, $CDCl_3$) δ (ppm): 169.6, 167.9, 166.8, 166.3, 110.6, 110.3, 56.4, 50.7, 47.4, 47.2, 33.5, 27.1, 26.1, 26.1. Note: in the ^{13}C NMR spectrum, the following pairs of peaks, 169.6 and 167.9, 166.8 and 166.3, 110.6 and 110.3, represent the same carbon in the two stereoisomers *E* and *Z*.

4.1.2. 1-Azabicyclo[2.2.2]octane-3-acetic acid methyl ester (37)—To a solution of 2-(1-azabicyclo[2.2.2]oct-3-ylidene)-acetic acid methyl ester (*Z*/*E* mixture) **36** (7.25 g, 40.0 mmol, 1 equiv) in methanol (500 mL), 10% Pd/C (725 mg) was added under an argon atmosphere. The resulting mixture was stirred at rt for 1 h under a balloon of hydrogen. The catalyst was filtered off over a celite pad, the celite was washed with methanol and the solvent was removed under vacuum. The residue was dissolved in dichloromethane (200 mL) and the solution was treated with 1 N HCl (200 mL). The organic layer was separated, and the residual aqueous phase was washed with dichloromethane (2 × 200 mL) and then basified to pH = 9 with Na_2CO_3 and extracted with dichloromethane (3 × 200 mL). The combined organic layers were dried over anhydrous Na_2SO_4, filtered and concentrated *in vacuo* to obtain compound **37**. Colorless oil; yield: 7.33 g, 100%; R_f = 0.19 (dichloromethane/methanol 7:3). ^{1}H NMR (300 MHz, $CDCl_3$) δ (ppm): 3.67 (s, 3H), 3.22–3.07 (m, 1H), 2.91–2.71 (m, 4H), 2.43–2.29 (m, 3H), 2.19–2.02 (m, 1H), 1.72–1.52 (m, 4H), 1.48–1.32 (m, 1H). ^{13}C NMR (75 MHz, $CDCl_3$) δ (ppm): 173.3, 54.7, 51.6, 47.7, 46.8, 38.5, 32.6, 28.1, 25.2, 21.2.

4.1.3. Borane 1-azabicyclo[2.2.2]octane-3-acetic acid methyl ester complex (38)—A 1.0 M solution of BH_3 in tetrahydrofuran (40 mL, 40.0 mmol, 1 equiv) was added dropwise via a syringe under an argon atmosphere to a stirred solution of 1-

azabicyclo[2.2.2]octane-3-acetic acid methyl ester **37** (7.33 g, 40.0 mmol, 1 equiv) in dry tetrahydrofuran (500 mL) at 0 °C. After stirring for 1.5 h at rt (TLC in dichloromethane/methanol 7:3), the mixture was quenched by addition of a saturated aqueous solution of $NaHCO_3$. Dichloromethane was added and the organic layer was separated. The aqueous layer was then extracted two more times with dichloromethane. The collected organic phases were dried over anhydrous Na_2SO_4, filtered and concentrated under reduced pressure affording the *N*-boranyl derivative **38.** Colorless solid; yield: 7.65 g, 97%; mp 87–88 °C; R_f = 0.30 (cyclohexane/ethyl acetate 4:1). ^{1}H NMR (300 MHz, $CDCl_3$) δ (ppm): 3.62 (s, 3H), 3.31–3.14 (m, 1H), 3.03–2.82 (m, 4H), 2.54–2.41 (m, 1H), 2.41–2.22 (m, 3H), 1.85–1.67 (m, 4H), 1.67–1.47 (m,1H). ^{13}C NMR (75 MHz, $CDCl_3$) δ (ppm): 172.1, 59.7, 53.5, 52.9, 51.8, 37.8, 31.5, 26.3, 24.8, 20.1.

4.1.4. General procedure for the synthesis of amidoximes (39–52)—In a pressurized sealed vial, aqueous hydroxylamine 50% w/w (4 equiv) was added to a stirred solution of the appropriate carbonitrile (1 equiv) in absolute ethanol. The resulting mixture was heated at 90 °C for 1 h. The solvent was then evaporated to dryness providing the desired amidoxime quantitatively, which was used without further purification.

4.1.4.1. 3-Fluoro-N′-hydroxybenzimidamide (39).: According to general procedure, hydroxylamine (2.29 mL, 37.42 mmol) was reacted with 3-fluorobenzonitrile (1.0 mL, 9.35 mmol) in absolute ethanol (8 mL) at 90 °C for 1 h to afford the desired compound **39.** Colorless oil; yield: 1.44 g, 100%; R_f = 0.51 (cyclohexane/ethyl acetate 1:1). ^{1}H NMR ($CDCl_3$, 300 MHz) δ (ppm): 7.64 (br s, 1H), 7.43–7.28 (m, 3H), 7.18–6.99 (m, 1H), 4.96 (br s, 2H). ^{13}C NMR ($CDCl_3$, 75 MHz) δ (ppm): 162.8 (d, J = 246.4 Hz), 151.9,134.7 (d, J = 8.1 Hz), 130.4 (d, J = 8.2 Hz), 121.7 (d, J = 3.0 Hz), 117.0 (d, J = 21.2 Hz), 113.2 (d, J = 23.4 Hz).

4.1.4.2. 3-Chloro-N′-hydroxybenzimidamide (40).: According to general procedure, hydroxylamine (2.67 mL, 43.62 mmol) was reacted with 3-chlorobenzonitrile (1.50 g, 10.90 mmol) in absolute ethanol (8 mL) at 90 °C for 1 h to afford the desired compound **40.** Colorless oil; yield: 1.86g, 100%; R_f = 0.51 (cyclohexane/ethyl acetate 1:1). ^{1}H NMR ($(CD_3)_2SO$, 300 MHz) δ (ppm): 9.77 (s, 1H), 7.73–7.69 (m, 1H), 7.65 (dt, J = 6.7, 1.8 Hz, 1H), 7.44–7.35 (m, 2H), 5.88 (s, 2H). ^{13}C NMR ($(CD_3)_2SO$, 75 MHz) δ (ppm): 149.6, 135.4, 132.9, 130.0, 128.6, 125.1, 123.9.

4.1.4.3. 3-Bromo-N′-hydroxybenzimidamide (41).: According to general procedure, hydroxylamine (2.02 mL, 32.96 mmol) was reacted with 3-bromobenzonitrile (1.50 g, 8.24 mmol) in absolute ethanol (8 mL) at 90 °C for 1 h to afford the desired compound **41.** Colorless oil; yield: 1.77 g, 100%; R_f = 0.51 (cyclohexane/ethyl acetate 1:1). ^{1}H NMR ($CDCl_3$, 300 MHz) δ (ppm): 7.75–7.69 (m, 1H), 7.53–7.45 (m, 2H), 7.20 (dd, J = 9.4, 6.4 Hz, 1H), 4.79 (br s, 2H). ^{13}C NMR ($CDCl_3$, 75 MHz) δ (ppm): 151.6, 134.6, 133.2, 130.3, 129.2, 124.6.122.9.

4.1.4.4. N′-Hydroxy-3-iodobenzimidamide (42).: According to general procedure, hydroxylamine (1.60 mL, 26.2 mmol) was reacted with 3-iodobenzonitrile (1.50 g, 6.55

mmol) in absolute ethanol (8 mL) at 90 °C for 1 h to afford the desired compound **42**. Colorless oil; yield: 1.72 g, 100%; R_f = 0.51 (cyclohexane/ethyl acetate 1:1). ^{1}H NMR ($CDCl_3$, 300 MHz) δ (ppm): 8.57 (br s, 1H), 7.97 (t, J = 1.7 Hz, 1H), 7.74 (ddd, J = 7.9, 1.7, 1.0 Hz, 1H), 7.58 (ddd, J = 7.8, 1.5, 1.1 Hz, 1H), 7.12 (t, J = 7.9 Hz, 1H), 4.91 (br s, 2H). ^{13}C NMR ($CDCl_3$, 75 MHz) δ (ppm): 151.6, 139.1, 135.0, 134.5, 130.4, 125.3, 94.5.

4.1.4.5. N′-Hydroxy-3-(trifluoromethyl)benzimidamide (43).: According to general procedure, hydroxylamine (430 μL, 7.1 mmol) was reacted with 3-(trifluoromethyl)benzonitrile (234 μL, 1.75 mmol) in absolute ethanol (6 mL) at 90 °C for 1.5 h to afford the desired compound **43**. Pale yellow oil; yield: 350 mg, 98%; R_f = 0.45 (cyclohexane/ethyl acetate 1:1). ^{1}H NMR ($CDCl_3$, 300 MHz) δ (ppm): 8.77 (br s,1H), 7.87–7.80 (m, 1H), 7.78–7.70 (m, 1H), 7.65–7.57 (m, 1H), 7.50–7.41 (m, 1H), 4.87 (br s, 2H). ^{13}C NMR ($CDCl_3$, 75 MHz) δ (ppm): 151.8, 133.4, 131.3 (d, J = 32.6 Hz), 129.4, 129.3, 126.8 (q, J = 3.7 Hz), 124.0 (q, J = 272.3 Hz), 123.1 (q, J = 3.9 Hz).

4.1.4.6. N′-Hydroxy-3-methylbenzimidamide (44).: According to general procedure, hydroxylamine (3.06 mL, 50.0 mmol) was reacted with 3-methylbenzonitrile (1.50 mL, 12.50 mmol) in absolute ethanol (8 mL) at 90 °C for 1 h to afford the desired compound **44.** Colorless oil; yield: 1.80 g, 96%; R_f = 0.46 (cyclohexane/ethyl acetate 1:1). ^{1}H NMR($CDCl_3$, 300 MHz) δ (ppm): 7.50–7.38 (m, 2H), 7.34–7.18 (m, 2H), 4.94 (br s, 2H), 2.37 (s, 3H). ^{13}C NMR ($CDCl_3$, 75 MHz) δ (ppm): 152.9, 138.4, 132.5, 130.8, 128.6, 126.7, 123.1, 21.5.

4.1.4.7. N′-Hydroxy-3-methoxybenzimidamide (45).: According to general procedure, hydroxylamine (1.84 mL, 30.04 mmol) was reacted with 3-methoxybenzonitrile (1.0 g, 7.51 mmol) in absolute ethanol (8 mL) at 90 °C for 1.5 h to afford the desired compound **45;** Colorless solid; yield: 1.22 g, 98%; mp 104–105 °C; R_f = 0.30 (cyclohexane/ethyl acetate 1:4). ^{1}H NMR($CDCl_3$, 300 MHz) δ (ppm): 7.39 (br s, 1H), 7.16–7.08 (m, 1H), 7.07–7.01 (m, 2H), 6.85–6.69 (m, 1H), 4.96 (br s, 2H), 3.63 (s, 3H). ^{13}C NMR ($CDCl_3$, 75 MHz) δ (ppm): 159.5, 152.9, 133.7, 129.6, 118.2, 115.9, 111.2, 55.2.

4.1.4.8. N′-Hydroxy-4-methoxybenzimidamide (46).: According to general procedure, hydroxylamine (1.84 mL, 30.04 mmol) was reacted with 4-methoxybenzonitrile (1.0 g, 7.51 mmol) in absolute ethanol (8 mL) at 90 °C for 1.5 h to afford the desired compound **46.** Colorless solid; yield: 1.21 g, 97%; mp 121–122 °C; R_f = 0.30 (cyclohexane/ethyl acetate 1:4). ^{1}H NMR($CDCl_3$, 300 MHz) δ (ppm): 7.57 (d, J = 8.9 Hz, 2H), 6.91 (d, J = 8.9 Hz, 2H), 4.90 (s, 2H), 3.83 (s, 3H). ^{13}C NMR ($CDCl_3$, 75 MHz) δ (ppm): 161.1, 152.7, 127.4, 125.1, 114.2, 55.5.

4.1.4.9. N′-Hydroxyfuran-2-carboximidamide (49).: According to general procedure, hydroxylamine (50% w/w in water, 790 μL, 12.89 mmol) was reacted with 2-furonitrile (282 μL, 3.22 mmol) in absolute ethanol (6 mL) at 90 °C for 1.5 h to afford the desired compound **49.** Colorless solid; yield: 400 mg, 99%; mp 57–58 °C; R_f = 0.32 (cyclohexane/ethyl acetate 1:1). ^{1}H NMR ($CDCl_3$, 300 MHz) δ (ppm): 8.67 (br s, 1H), 7.30 (dd, J = 1.7, 0.7 Hz, 1H),

6.69 (dd, J = 3.4, 0.6 Hz, 1H), 6.29 (dd, J = 3.5, 1.8 Hz, 1H), 5.05 (br s, 2H). ^{13}C NMR ($CDCl_3$, 75 MHz) δ (ppm): 145.9, 145.5, 142.9, 111.6, 108.4.

4.1.4.10. Thiophene-2-amidoxime (50).: According to general procedure, hydroxylamine (50% w/w in water, 2.63 mL, 42.96 mmol) was reacted with 2-thiophenecarbonitrile (1.0 mL, 10.74 mmol) in absolute ethanol (8 mL) at 90 °C for 1.5 h to afford the desired compound **50**. Colorless solid; yield: 1.53 g, 100%; mp 90–96 °C; R_f = 0.52 (cyclohexane/ethyl acetate 1:1). ^{1}H NMR ($CDCl_3$, 300 MHz) δ (ppm): 7.52–7.08 (m, 3H), 7.01 (dd, J = 4.9, 3.9 Hz, 1H), 4.98 (br s, 2H). ^{13}C NMR ($CDCl_3$, 75 MHz) δ (ppm): 148.6, 134.9, 127.2, 126.8, 125.3.

4.1.4.11. N'-Hydroxyacetimidamide (52).: According to general procedure, hydroxylamine (50% w/w in water, 25.0 mL, 384.0 mmol) was reacted with acetonitrile (5.0 mL, 96.0 mmol) in absolute ethanol (50 mL) at 90 °C for 3 h. The desired acetamidoxime **52** was recrystallized from propan-2-ol. Colorless solid; yield: 7.10 g, 100%; mp 134–136°C; R_f = 0.54 (CH_2Cl_2/MeOH 4:1). ^{1}H NMR ((CD_3)$_2$SO, 300 MHz) δ (ppm): 8.76 (br s, 1H), 5.33 (br s, 2H), 1.62 (s, 3H). ^{13}C NMR ((CD3)2SO, 75 MHz) δ (ppm): 149.6, 16.7.

4.1.5. General procedure for the synthesis of boranyl intermediates (53–65)

Method A.: Cesium carbonate (3 equiv) was added to a suspension of the appropriate amidoxime (3 equiv) in tetrahydrofuran. The mixture was heated at 50 °C for 20 min and then cooled to rt before adding, dropwise via a syringe, a solution of methyl ester (1 equiv) in tetrahydrofuran. The final mixture was stirred for 12 h at 80 °C (TLC in dichloromethane/methanol 7:3) and then standard workup was applied.

Method B.: In anhydrous conditions, under an atmosphere of argon and in presence of 3 Å molecular sieves, the appropriate amidoxime (3 equiv) was suspended in dry tetrahydrofuran and stirred at rt for 30 min. 60% NaH dispersion in mineral oil (3 equiv) was then added portionwise and the resulting reaction mixture was heated at 50 °C for 20 min. A solution of methyl ester (1 equiv) in dry tetrahydrofuran was subsequently added dropwise via a syringe at rt and the final suspension was stirred for 2 h at 80 °C (TLC in dichloromethane/methanol 7:3). Standard workup was then applied.

Standard workup.: The reaction was quenched with saturated aqueous solution of $NaHCO_3$ and diluted with dichloromethane. The mixture was acidified with 1 N HCl (pH = 1), the organic phase removed and then extracted two more times with 1 N HCl. The combined aqueous layers were basified with Na_2CO_3 and extracted with dichloromethane (× 3). Alternatively, the reaction mixture was directly extracted three times with dichloromethane. Upon complete extraction, the organic phases were combined, dried over anhydrous Na_2SO_4, filtered and concentrated under vacuum. The residue was purified by silica gel column chromatography.

4.1.5.1. Borane 3-(3-fluorophenyl)-5-(quinuclidin-3-ylmethyl)-1,2,4-oxadiazole complex (53).: Following method A, methyl ester **38** (500 mg, 2.54 mmol) was reacted with 3-fluoro-*N*'-hydroxy-benzimidamide **39** (1.17 g, 7.61 mmol) and Cs_2CO_3 (2.48 g, 7.61

mmol). Standard workup and silica gel column chromatography gained the desired compound. Pale yellow oil; yield: 589 mg, 77%; R_f = 0.43 (cyclohexane/ethyl acetate 7:3). ^{1}H NMR($CDCl_3$, 300 MHz) δ (ppm): 7.82–7.75 (m, 1H), 7.69 (ddd, J = 9.4, 2.6, 1.5 Hz, 1H), 7.39 (td, J = 8.0, 5.7 Hz, 1H), *7.14* (tdd, J = 8.4, 2.6, 1.0 Hz, 1H), 3.39–3.24 (m, 1H), 3.09–2.87 (m, 6H), 2.62 (ddd, J = 13.6, 6.9, 2.0 Hz, 1H), 2.57–2.43 (m,1H), 1.97–1.85 (m, 2H), 1.85–1.74 (m, 2H), 1.74–1.59 (m, 1H). ^{13}C NMR ($CDCl_3$, 75 MHz) δ (ppm): 177.8, 167.6, 162.9 (d, J = 246.7 Hz), 130.7 (d, J = 8.1 Hz), 128.6 (d, J = 8.6 Hz), 123.2 (d, J = 3.2 Hz), 118.4 (d, J = 21.2 Hz), 114.5 (d, J = 23.7 Hz), 59.4, 53.6, 52.9, 33.1, 30.1, 26.2, 24.6, 20.0.

4.1.5.2. Borane 3-(3-chlorophenyl)-5-(quinuclidin-3-ylmethyl)-1,2,4-oxadiazole complex (54).: Following method A, methyl ester **38** (400 mg, 2.03 mmol) was reacted with 3-chloro-*N*′-hydroxybenzimidamide **40** (1.04 g, 6.09 mmol) and Cs_2CO_3 (1.98 g, 6.09 mmol). Standard workup and silica gel column chromatography gained the desired compound. Colorless solid; yield: 609 mg, 95%; mp 159–160 °C; R_f = 0.42 (cyclohexane/ethyl acetate 7:3). ^{1}H NMR ($CDCl_3$, 300 MHz) δ (ppm): 8.01–7.97 (m, 1H), 7.88 (dt, J = 7.5, 1.5 Hz, 1H), 7.42 (ddd, J = 8.1, 2.0,1.4 Hz, 1H), 7.35 (t, J = 7.8 Hz, 1H), 3.39–3.24 (m, 1H), 3.09–2.86 (m, 6H), 2.61 (ddd, J = 13.6, 6.9, 2.1 Hz, 1H), 2.57–2.42 (m, 1H), 1.99–1.85 (m, 2H), 1.85–1.73 (m, 2H), 1.73–1.59 (m, 1H). ^{13}C NMR ($CDCl_3$, 75 MHz) δ (ppm): 177.9, 167.6, 135.1, 131.5, 130.4, 128.4, 127.7, 125.6, 59.5, 53.7, 53.0, 33.2, 30.2, 26.3, 24.7, 20.1.

4.1.5.3. Borane 3-(3-bromophenyl)-5-(quinuclidin-3-ylmethyl)-1,2,4-oxadiazole complex (55).: Following method A, methyl ester **38** (300 mg, 1.52 mmol) was reacted with 3-bromo-*N*′-hydroxybenzimidamide **41** (982 mg, 4.57 mmol) and Cs_2CO_3 (1.49 g, 4.57 mmol). Standard workup and silica gel column chromatography gained the desired compound. Colorless solid; yield: 490 mg, 89%; mp 155–156 °C; R_f = 0.42 (cyclohexane/ethyl acetate 7:3). ^{1}H NMR ($CDCl_3$, 300 MHz) δ (ppm): 8.15 (t, J = 1.8 Hz, 1H), 7.96–7.89 (m, 1H), 7.57 (ddd, J = 8.0, 2.0, 1.0 Hz, 1H), 7.29 (t, J = 7.9 Hz, 1H), 3.38–3.23 (m, 1H), 3.07–2.87 (m, 6H), 2.62 (ddd, J = 13.7, 6.9, 2.1 Hz, 1H), 2.57–2.41 (m, 1H), 1.99–1.85 (m, 2H), 1.85–1.73 (m, 2H), 1.73–1.58 (m, 1H). ^{13}C $_{NMR(CDC}1_3$, 75 MHz) δ (ppm): 177.9, 167.5, 134.4, 130.6, 128.7, 126.1, 123.1, 59.6, 53.7, 53.1, 33.3, 30.3, 26.4, 24.8, 20.2.

4.1.5.4. Borane 3-(3-iodophenyl)-5-(quinuclidin-3-ylmethyl)-1,2,4-oxadiazole complex (56).: Following method A, methyl ester **38** (500 mg, 2.54 mmol) was reacted with *N*′-hydroxy-3-iodobenzimidamide **42** (1.99 g, 7.61 mmol) and Cs_2CO_3 (2.48 g, 7.61 mmol). Standard workup and silica gel column chromatography gained the desired compound. Pale yellow oil; yield: 873 mg, 84%; R_f = 0.43 (cyclohexane/ethyl acetate 7:3). ^{1}H NMR ($CDCl_3$, 300 MHz) δ (ppm): 8.37–8.32 (m, 1H), 7.99–7.93 (m, 1H), 7.82–7.73 (m, 1H), 7.19–7.11 (m, 1H), 3.38–3.23 (m, 1H), 3.09–2.86 (m, *6*H), 2.61 (ddd, J = 13.6, 6.9, 1.7 Hz, 1H), 2.56–2.42 (m, 1H), 1.98–1.85 (m, 2H), 1.85–1.74 (m, 2H), 1.74–1.59 (m, 1H). ^{13}C NMR ($CDCl_3$, 75 MHz) δ (ppm): 177.8, 167.2, 140.3, 136.3, 130.6, 128.6, 126.6, 94.5, 59.5, 53.6, 53.0, 33.2, 30.2, 26.3, 24.7, 20.1.

4.1.5.5. Borane 5-(quinuclidin-3-ylmethyl)-3-(3-(trifluoromethyl) phenyl)-1,2,4-oxadiazole complex (57).: Following method B, methyl ester **38** (421 mg, 2.14 mmol) was reacted with *N*'-hydroxy-3-(trifluoromethyl)-benzimidamide **43** (1.31 g, 6.41 mmol) and 60% NaH dispersion in mineral oil (256 mg, 6.41 mmol). Standard workup and silica gel column chromatography (cyclohexane/ethyl acetate 3:2 to 1:1) gained the desired compound. Pale yellow oil; yield: 355 mg, 47%; R_f = 0.63 (cyclohexane/ethyl acetate 1:1). ^{1}H NMR ($CDCl_3$, 300 MHz) δ (ppm): 8.29–8.22 (m, 1H), 8.21–8.14 (m, 1H), 7.69 (dd, *J* = 7.9, 0.5 Hz, 1H), 7.55 (t, *J* = 7.8 Hz, 1H), 3.37–3.23 (m, 1H), 3.07–2.86 (m, 6H), 2.61 (ddd, *J* = 13.5, 6.9, 1.9 Hz, 1H), 2.57–2.43 (m, 1H), 1.97–1.85 (m, 2H), 1.85–1.73 (m, 2H), 1.73–1.58 (m, 1H). ^{13}C NMR ($CDCl_3$, 75 MHz) δ (ppm): 178.1, 167.5, 131.6 (q, *J* = 32.9 Hz), 130.7, 129.6, 128.0 (q, *J* = 3.8 Hz), 127.6, 124.5 (q, *J* = 3.9 Hz), 123.8 (q, *J* = 272.6 Hz), 59.5, 53.6, 53.0, 33.2, 30.2, 26.3, 24.7, 20.1.

4.1.5.6. Borane 5-(quinuclidin-3-ylmethyl)-3-(m-tolyl)-1,2,4-oxadiazole complex (58).: Following general method A, methyl ester **38** (300 mg, 1.52 mmol) was reacted with *N*'-hydroxy-3-methylbenzimidamide **44** (686 mg, 4.57 mmol) and Cs_2CO_3 (1.49 g, 4.57 mmol). Standard workup and silica gel column chromatography (cyclohexane/ethyl acetate 3:2 to 1:1) gained the desired compound. Pale yellow oil; yield: 406 mg, 90%; R_f = 0.51 (cyclohexane/ethyl acetate 7:3). ^{1}H NMR($CDCl_3$, 300 MHz) δ (ppm): 7.83–7.74 (m, 2H), 7.34–7.21 (m, 2H), 3.37–3.22 (m, 1H), 3.06–2.86 (m, 6H), 2.61 (ddd, *J* = 13.7, 6.9, 2.0 Hz, 1H), 2.56–2.42 (m, 1H), 2.35 (s, 3H), 1.96–1.81 (m, 2H), 1.81–1.71 (m, 2H), 1.71–1.55 (m, 1H). ^{13}C NMR ($CDCl_3$, 75 MHz) δ (ppm): 177.4, 168.6, 138.8, 132.2, 128.9, 128.1, 126.5, 124.7, 59.5, 53.6, 53.0, 33.3, 30.2, 26.3, 24.7, 21.4, 20.1.

4.1.5.7. Borane 3-(3-methoxyphenyl)-5-(quinuclidin-3-ylmethyl)-1.2.4-oxadiazole complex (59).: Following method A, methyl ester **38** (500 mg, 2.54 mmol) was reacted with *N*'-hydroxy-3-methoxybenzimidamide **45** (1.26 g, 7.61 mmol) and Cs_2CO_3 (2.48 g, 7.61 mmol). Standard workup and silica gel column chromatography (cyclohexane/ethyl acetate 4:1 to 3:2) gained the desired compound. Colorless oil; yield: 487 mg, 61%; R_f = 0.39 (cyclohexane/ethyl acetate 7:3). ^{1}H NMR($CDCl_3$, 300 MHz) δ (ppm): 7.58 (dt, *J* = 7.7, 1.1 Hz, 1H), 7.50 (dd, *J* = 2.5, 1.5 Hz, 1H), 7.32 (t, *J* = 8.0 Hz, 1H), 6.98 (ddd, *J* = 8.3, 2.6, 0.9 Hz, 1H), 3.80 (s, 3H), 3.36–3.21 (m, 1H), 3.05–2.85 (m, *6*H), 2.61 (ddd, *J* = 13.6, 6.9, 1.9 Hz, 1H), 2.56–2.42 (m, 1H), 1.97–1.82 (m, 2H), 1.82–1.72 (m, 2H), 1.72–1.56 (m, 1H). ^{13}C NMR (*CDC*1_3, 75 MHz) δ (ppm): 177.5, 168.1, 159.7, 129.9, 127.6, 119.7, 117.4, 112.0, 59.2, 55.3, 53.4, 52.8, 32.9, 29.9, 26.0, 24.4, 19.8.

4.1.5.8. Borane 3-(4-methoxyphenyl)-5-(quinuclidin-3-ylmethyl)-1.2.4-oxadiazole complex (60).: Following method A, methyl ester **38** (152 mg, 0.77 mmol) was reacted with *N*'-hydroxy-4-methoxybenzimidamide **46** (384 mg, 2.31 mmol) and Cs_2CO_3 (753 mg, 2.31 mmol). Standard workup and silica gel column chromatography (cyclohexane/ethyl acetate 4:1 to 3:2) gained the desired compound. Yellow oil; yield: 75 mg, 31%; R_f = 0.43 (cyclohexane/ethyl acetate 1:4). ^{1}H NMR ($CDCl_3$, 300 MHz) δ (ppm): 7.92 (d, *J* = 8.9 Hz, 2H), 6.92 (d, *J* = 9.0 Hz, 2H), 3.80 (s, 3H), 3.36–3.24 (m, 1H), 3.04–2.88 (m, *6*H), 2.62 (ddd, *J* = 13.7, 7.0, 2.1Hz, 1H), 2.56–2.43 (m, 1H), 1.99–1.82 (m, 2H), 1.82–1.72 (m, 2H),

1.72–1.57 (m, 1H). ^{13}C NMR ($CDCl_3$, 75 MHz) δ (ppm): 177.2, 168.2, 162.2, 129.2, 119.1, 114.4, 59.6, 55.5, 53.7, 53.0, 33.3, 30.2, 26.3, 24.7, 20.1.

4.1.5.9. Borane 3-(pyridin-3-yl)-5-(quinuclidin-3-ylmethyl)-1,2,4-oxadiazole complex (61).: Following method B, methyl ester **38** (350 mg, 1.78 mmol) was reacted with 3-pyridylamidoxime **47** (731 mg, 5.33 mmol) and 60% NaH dispersion in mineral oil (213 mg, 5.33 mmol). Standard workup and silica gel column chromatography gained the desired compound. Yellow oil; yield: 258 mg, 51%; R_f = 0.28 (cyclohexane/ethyl acetate 1:1). ^{1}H NMR ($CDCl_3$, 300 MHz) δ (ppm): 9.22 (d, J = 2.1 Hz, 1H), 8.68 (dd, J = 4.9, 1.7 Hz, 1H), 8.26 (dt, J = 8.0,1.9 Hz, 1H), 7.37 (dd, J = 7.9, 4.9 Hz, 1H), 3.38–3.25 (m, 1H), 3.10–2.87 (m, 6H), 2.62 (ddd, J = 13.5, 6.9, 2.0 Hz, 1H), 2.57–2.43 (m, 1H), 1.99–1.86 (m, 2H), 1.86–1.75 (m, 2H), 1.75–1.56 (m, 1H). ^{13}C NMR ($CDCl_3$, 75 MHz) δ (ppm): 178.0, 166.4, 152.1, 148.5, 134.6, 123.7, 122.8, 59.3, 53.5, 52.8, 33.0, 30.0, 26.1, 24.6, 19.9.

4.1.5.10. Borane 3-(pyridin-4-yl)-5-(quinuclidin-3-ylmethyl)-1,2,4-oxadiazole complex (62).: Following method B, methyl ester **38** (350 mg, 1.78 mmol) was reacted with 4-pyridylamidoxime **48** (731 mg, 5.33 mmol) and 60% NaH dispersion in mineral oil (213 mg, 5.33 mmol). Standard workup and silica gel column chromatography (cyclohexane/ethyl acetate 1:1) gained the desired compound. Yellow oil; yield: 392 mg, 78%; R_f = 0.33 (cyclohexane/ethyl acetate 3:7). ^{1}H NMR ($(CD_3)_2SO$, 300MHz) δ (ppm): 8.79 (dd, J = 4.5, 1.6 Hz, 2H), 7.91 (dd, J = 4.4, 1.7 Hz, 2H), 3.29–3.08 (m, 3H), 2.99–2.74 (m, 4H), 2.66–2.54 (m, 1H), 2.53–2.38 (m, 1H), 1.98–1.78 (m, 1H), 1.78–1.65 (m, 2H), 1.64–1.42 (m, 2H). ^{13}C NMR ($(CD_3)_2SO$, 75 MHz) δ (ppm): 179.9, 166.2, 150.9, 133.5, 120.9, 58.7, 53.0, 52.4, 32.3, 29.1, 25.4, 24.1,19.3.

4.1.5.11. Borane 3-(furan-2-yl)-5-(quinuclidin-3-ylmethyl)-1,2,4-oxadiazole complex (63).: Following method A, methyl ester **38** (200 mg, 1.01 mmol) was reacted with *N*′-hydroxyfuran-2-carboxyimidamide **49** (384 mg, 3.04 mmol) and Cs_2CO_3 (992 mg, 3.04 mmol). Standard workup and silica gel column chromatography (cyclohexane/ethyl acetate 7:3 to 3:2) gained the desired compound. Yellow oil; yield: 158 mg, 57%; R_f = 0.24 (cyclohexane/ethyl acetate 7:3). ^{1}H NMR ($CDCl_3$, 300 MHz) δ (ppm): 7.55 (dd, J = 1.8, 0.8 Hz, 1H), 7.05 (dd, J = 3.5, 0.5 Hz, 1H), 6.50 (dd, J = 3.3, 1.8 Hz, 1H), 3.36–3.22 (m, 1H), 3.06–2.86 (m, 6H), 2.59 (ddd, J = 13.5, 7.0, 2.1Hz, 1H), 2.55–2.41 (m, 1H), 1.95–1.83 (m, 2H), 1.83–1.72 (m, 2H), 1.72–1.57 (m, 1H). ^{13}C NMR ($CDCl_3$, 75 MHz) δ (ppm): 177.6, 161.5, 145.4, 142.1, 114.1, 112.0, 59.4, 53.6, 53.0, 33.2, 30.1, 26.3, 24.7, 20.1.

4.1.5.12. Borane 5-(quinuclidin-3-ylmethyl)-3-(thiophen-2-yl)-1,2,4-oxadiazole complex (64).: Following method B, methyl ester **38** (350 mg, 1.78 mmol) was reacted with thiophene-2-amidoxime **50** (758 mg, 5.33 mmol) and 60% NaH dispersion in mineral oil (213 mg, 5.33 mmol). Standard workup and silica gel column chromatography (cyclohexane/ethyl acetate 85:15) gained the desired compound. Pale yellow oil; yield: 336 mg, 65%; R_f = 0.39 (cyclohexane/ethyl acetate 7:3). ^{1}H NMR($CDCl_3$, 300 MHz) δ (ppm): 7.71 (dd, J = 3.7, 1.2 Hz, 1H), 7.44 (dd, J = 5.0, 1.2 Hz, 1H), 7.09 (dd, J = 5.0, 3.7 Hz, 1H), 3.37–3.21 (m, 1H), 3.07–2.85 (m, 6H), 2.60 (ddd, J = 13.6, 7.0, 2.1 Hz, 1H), 2.55–2.41 (m, 1H), 1.98–1.84 (m, 2H), 1.84–1.72 (m, 2H), 1.72–1.53 (m, 1H). ^{13}C NMR ($CDCl_3$, 75

MHz) δ (ppm): 177.5, 164.5, 129.7, 129.5, 128.1, 128.0, 59.3, 53.5, 52.9, 33.1, 30.0, 26.1, 24.6, 20.0.

4.1.5.13. Borane 3-phenyl-5-(quinuclidin-3-ylmethyl)-1,2,4-oxadiazole complex (65).: Following method A, methyl ester **38** (500 mg, 2.54 mmol) was reacted with benzamidoxime **51** (1.04 g, 7.61 mmol) and Cs_2CO_3 (2.48 g, 7.61 mmol). Standard workup and silica gel column chromatography gained the desired compound. Colorless solid; yield: 370 mg, 51%; mp 129–131 °C; R_f = 0.42 (cyclohexane/ethyl acetate 7:3). ^{1}H NMR ($CDCl_3$, 300 MHz) δ (ppm): 8.03–7.95 (m, 2H), 7.48–7.37 (m, 3H), 3.36–3.24 (m, 1H), 3.06–2.87 (m, 6H), 2.62 (ddd, J = 13.7, 7.0, 2.0 Hz, 1H), 2.57–2.43 (m, 1H), 1.95–1.84 (m, 2H), 1.84–1.72 (m, 2H), 1.72–1.57 (m, 1H). ^{13}C NMR ($CDCl_3$, 75 MHz) δ (ppm): 177.5, 168.2, 131.2, 128.8, 127.3, 126.5, 59.3, 53.4, 52.8, 32.9, 30.00, 26.0, 24.5, 19.8.

4.1.6. General procedure for borane complex cleavage (21–33)—Under argon atmosphere and at 0 °C, a solution of CF_3COOH (5 equiv) in acetone (3.5 mL/mmol) was added dropwise to a solution of the appropriate 1,2,4-oxadiazole intermediate (**53–65**) (1 equiv) in acetone (3.5 mL/mmol). The resulting mixture was allowed to stir overnight at rt (TLC in cyclohexane/ethyl acetate 2:3 or dichloromethane/methanol 95:5) and then was concentrated under reduced pressure. The residue was diluted with deionized water and the aqueous solution (pH = 1–2) was extracted once with diethyl ether. The aqueous phase was then basified with Na_2CO_3 and extracted three times with dichloromethane. The dichloromethane organic phases were combined, dried over anhydrous Na_2SO_4, filtered and evaporated to dryness to afford the pure compound, which was used without further purification.

4.1.6.1. 3-(3-Fluorophenyl)-5-(quinuclidin-3-ylmethyl)-1,2,4-oxadiazole (21).: Applying the general procedure, **53** (589 mg, 1.96 mmol, 1 equiv) was treated with CF_3COOH (753 μL, 9.78 mmol) in acetone. After disappearance of the starting material (TLC in cyclohexane/ethyl acetate 1:1), standard workup provided the desired compound **21**. Yellow oil; yield: 529 mg, 94%; R_f = 0.48 (dichloromethane/methanol 95:5, alumina). ^{1}H NMR ($CDCl_3$, 300 MHz) δ (ppm): 7.79–7.72 (m, 1H), 7.65 (ddd, J = 9.5, 2.5, 1.5 Hz, 1H), 7.33 (td, J = 8.1, 5.8 Hz, 1H), 7.07 (tdd, J = 8.4, 2.6, 0.9 Hz, 1H), 3.17–3.03 (m, 1H), 2.89 (d, J = 7.9 Hz, 2H), 2.84–2.62 (m, 4H), 2.39 (ddd, J = 13.7, 6.2, 1.8 Hz, 1H), 2.25–2.09 (m, 1H), 1.73–1.57 (m, 2H), 1.57–1.43 (m, 2H), 1.43–1.28 (m, 1H). ^{13}C NMR ($CDCl_3$, 75 MHz) δ (ppm): 179.0, 167.2, 162.6 (d, J = 246.7 Hz), 130.4 (d, J = 8.2 Hz), 128.7 (d, J = 8.6 Hz), 122.9 (d, J = 3.1 Hz), 117.8 (d, J = 21.2 Hz), 114.2 (d, J = 23.6 Hz), 54.3, 47.4, 46.6, 34.0, 30.4, 27.7, 24.8, 20.7.

4.1.6.2. 3-(3-Chlorophenyl)-5-(quinuclidin-3-ylmethyl)-1,2,4-oxadiazole (22).: Applying the general procedure, **54** (609 mg, 1.92 mmol) was treated with CF_3COOH (740 μL, 9.59 mmol) in acetone. After disappearance of the starting material (TLC in cyclohexane/ethyl acetate 1:1), standard workup provided the desired compound **22**. Colorless solid; yield: 531 mg, 91%; mp 91–93 °C; R_f = 0.57 (dichloromethane/methanol 9:1, alumina). ^{1}H NMR ($CDCl_3$, 300 MHz) δ (ppm): 8.04–7.96 (m, 1H), 7.94–7.84 (m, 1H), 7.45–7.28 (m, 2H), 3.21–3.06 (m, 1H), 2.94 (d, J = 7.8 Hz, 2H), 2.88–2.67 (m, 4H), 2.50–

2.37 (m, 1H), 2.23 (dd, J = 15.4, 7.4 Hz, 1H), 1.80–1.49 (m, 4H), 1.49–1.32 (m, 1H). ^{13}C NMR ($CDCl_3$, 75 MHz) δ (ppm): 179.2, 167.3, 134.9, 131.2, 130.2, 128.6, 127.5, 125.4, 54.6, 47.7, 46.8, 34.3, 30.6, 28.0, 25.0, 20.9.

4.1.6.3. 3-(3-Bromophenyl)-5-(quinuclidin-3-ylmethyl)-1,2,4-oxadiazole (23).: Applying the general procedure, **55** (490 mg, 1.35 mmol) was reacted with CF_3COOH (521 μL, 6.77 mmol) in acetone. After disappearance of the starting material (TLC in cyclohexane/ethyl acetate 1:1), standard workup provided the desired compound **23**. Colorless solid; yield: 400 mg, 85%; mp 108–109 °C; R_f = 0.51 (dichloromethane/methanol 9:1, alumina). ^{1}H NMR ($CDCl_3$, 300 MHz) δ (ppm): 8.19–8.14 (m, 1H), 7.97–7.90 (m, 1H), 7.60–7.52 (m, 1H), 7.28 (t, J = 7.9 Hz, 1H), 3.21–3.07 (m, 1H), 2.94 (d, J = 7.9 Hz, 2H), 2.89–2.68 (m, 4H), 2.43 (ddd, J = 13.7, 6.2, 1.1 Hz, 1H), 2.30–2.15 (m, 1H), 1.86–1.48 (m, 4H), 1.49–1.33 (m, 1H). ^{13}C NMR ($CDCl_3$, 75 MHz) δ (ppm): 179.3, 167.3, 134.2, 130.5, 128.9, 126.0, 123.0, 54.6, 47.7, 46.9, 34.3, 30.7, 28.1, 25.0, 21.0.

4.1.6.4. 3-(3-Iodophenyl)-5-(quinuclidin-3-ylmethyl)-1,2,4-oxadiazole (24).: Applying the general procedure, **56** (873 mg, 2.13 mmol) was reacted with CF_3COOH (822 μL, 10.67 mmol) in acetone. After disappearance of the starting material (TLC in cyclohexane/ethyl acetate 1:1), standard workup provided the desired compound **24**. Colorless solid; yield: 768 mg, 91%; mp 149–151 °C; R_f = 0.50 (dichloromethane/methanol 95:5, alumina). ^{1}H NMR ($CDCl_3$, 300 MHz) δ (ppm): 8.44–8.40 (m, 1H), 8.06–7.99 (m, 1H), 7.85–7.79 (m, 1H), 7.24–7.16 (m, 1H), 3.20 (dd, J = 13.5, 9.8 Hz, 1H), 3.00 (d, J = 7.9 Hz, 2H), 2.95–2.74 (m, 4H), 2.49 (ddd, J = 13.7, 6.2, 1.8 Hz, 1H), 2.35–2.20 (m, 1H), 1.84–1.72 (m, 1H), 1.72–1.55 (m, 3H), 1.55–1.39 (m, 1H). ^{13}C NMR ($CDCl_3$, 75 MHz) δ (ppm): 179.3, 167.1, 140.2, 136.3, 130.6, 128.9, 126.6, 94.5, 54.7, 47.8, 47.0, 34.4, 30.8, 28.1, 25.1, 21.1.

4.1.6.5. 5-(Quinuclidin-3-ylmethyl)-3-(3-(trifluoromethyl)phenyl)-1,2,4-oxadiazole (25).: Applying the general the procedure, **57** (355 mg, 1.01 mmol) was treated with CF_3COOH (389 μL, 5.05 mmol) in acetone. After disappearance of the starting material (TLC in cyclohexane/ethyl acetate1:1), standard workup provided the desired compound **25**. Yellow oil; yield: 340 mg, 100%; R_f = 0.55 (dichloromethane/methanol 9:1, alumina). ^{1}H NMR ($CDCl_3$, 300 MHz) δ (ppm): 8.30–8.22 (m, 1H), 8.17 (d, J = 7.8 Hz, 1H), 7.66 (d, J = 7.9 Hz, 1H), 7.51 (t, J = 7.8 Hz, 1H), 3.13 (dd, J = 13.5, 9.9 Hz, 1H), 2.94 (d, J = 7.8 Hz, 2H), 2.87–2.66 (m, 4H), 2.43 (ddd, J = 13.7, 6.2, 1.7 Hz, 1H), 2.31–2.14 (m, 1H), 1.78–1.48 (m, 4H), 1.48–1.30 (m, 1H). ^{13}C NMR ($CDCl_3$, 75 MHz) δ (ppm): 179.4, 167.3, 131.5 (q, J = 32.9 Hz), 130.6, 129.5, 127.8, 127.7 (q, J = 3.7 Hz), 124.4 (q, J = 3.8 Hz), 123.8 (q, J = 272.4 Hz), 54.5, 47.6, 46.8, 34.3, 30.6, 27.9, 25.0, 20.9.

4.1.6.6. 5-(Quinuclidin-3-ylmethyl)-3-(m-tolyl)-1,2,4-oxadiazole (26).: Applying the general procedure, **58** (406 mg, 1.37 mmol) was reacted with CF_3COOH (526 μL, 6.83 mmol) in acetone. After disappearance of the starting material (TLC in cyclohexane/ethyl acetate 1:1), standard workup provided the desired compound **26**. Yellow oil; yield: 357 mg, 92%; R_f = 0.33 (dichloromethane/methanol 94:6, alumina). ^{1}H NMR ($CDCl_3$, 300 MHz) δ (ppm): 7.82–7.72 (m, 2H), 7.33–7.20 (m, 2H), 3.72–3.57 (m, 1H), 3.49–2.97 (m, 7H), 2.75–2.58 (m, 1H), 2.34 (s, 3H), 2.18–2.01 (m, 2H), 2.01–1.89 (m, 2H), 1.89–1.74 (m, 1H). ^{13}C

NMR ($CDCl_3$, 75 MHz) δ (ppm): 176.9, 168.5, 138.8, 132.2, 128.9, 128.0, 126.2, 124.5, 51.8, 46.4, 45.8, 31.7, 29.6, 24.2, 24.2, 21.4, 18.3.

4.1.6.7. 3-(3-Methoxyphenyl)-5-(quinuclidin-3-ylmethyl)-1,2,4-oxadiazole (27).: Applying the general procedure, **59** (755 mg, 2.41 mmol) was treated with CF_3COOH (923 μL, 12.05 mmol) in acetone. After disappearance of the starting material (TLC in cyclohexane/ethyl acetate 3:2), standard workup provided the desired compound **27**. Yellow oil; yield: 505 mg, 70%; R_f = 0.30 (dichloromethane/methanol 95:5, alumina). ^{1}H NMR ($CDCl_3$, 300 MHz) δ (ppm): 7.58 (dt, J = 7.7, 1.1 Hz, 1H), 7.51 (dd, J = 2.6, 1.5 Hz, 1H), 7.30 (t, J = 8.0 Hz, 1H), 6.96 (ddd, J = 8.3, 2.6, 1.0 Hz, 1H), 3.79 (s, 3H), 3.22–3.07 (m, 1H), 2.93 (d, J = 7.8 Hz, 2H), 2.88–2.67 (m, 4H), 2.44 (ddd, J = 13.7, 6.3, 1.7 Hz, 1H), 2.30–2.15 (m, 1H), 1.77–1.62 (m, 2H), 1.62–1.48 (m, 2H), 1.48–1.33 (m, 1H). ^{13}C NMR ($CDCl_3$, 75 MHz) δ (ppm): 178.8, 168.3, 159.9, 130.0, 128.0, 119.9, 117.6, 112.0, 55.5, 54.5, 47.6, 46.8, 34.2, 30.6, 27.9, 25.0, 20.8.

4.1.6.8. 3-(4-Methoxyphenyl)-5-(quinuclidin-3-ylmethyl)-1,2,4-oxadiazole (28).: Applying the general procedure, **60** (61 mg, 0.19 mmol) was treated with CF_3COOH (73 μL, 0.95 mmol) in acetone. After disappearance of the starting material (TLC in cyclohexane/ethyl acetate 3:2), standard workup provided the desired compound **28**. Yellow oil; yield: 57 mg, 100%; R_f = 0.30 (dichloromethane/methanol 95:5, alumina). ^{1}H NMR ($CDCl_3$, 300 MHz) δ (ppm): 7.93 (d, J = 8.9 Hz, 2H), 6.91 (d, J = 8.9 Hz, 2H), 3.79 (s, 3H), 3.24–3.07 (m, 1H), 2.93 (d, J = 7.9 Hz, 2H), 2.88–2.67 (m, 4H), 2.52–2.41 (m, 1H), 2.32–2.18 (m, 1H), 1.82–1.64 (m, 2H), 1.64–1.36 (m, 3H). ^{13}C NMR ($CDCl_3$, 75 MHz) δ (ppm): 178.5, 168.1, 162.0, 129.1, 119.3, 114.4, 55.5, 54.2, 47.5, 46.7, 34.1, 30.6, 27.7, 24.9, 20.7.

4.1.6.9. 3-(Pyridin-3-yl)-5-(quinuclidin-3-ylmethyl)-1,2,4-oxadiazole (29).: Applying the general procedure, **61** (258 mg, 0.91 mmol) was treated with CF_3COOH (351 μL, 4.55 mmol) in acetone. After disappearance of the starting material (TLC in cyclohexane/ethyl acetate 1:1), standard workup provided the desired compound **29**. Yellow oil; yield: 225 mg, 92%; R_f = 0.30 (dichloromethane/methanol 85:15, alumina). ^{1}H NMR ($CDCl_3$, 300 MHz) δ (ppm): 9.23 (d, J = 2.0 Hz, 1H), 8.70–8.63 (m, 1H), 8.27 (dt, J = 8.0, 2.0 Hz, 1H), 7.35 (ddd, J = 8.1, 4.9, 0.8 Hz, 1H), 3.21 −3.07 (m, 1H), 2.96 (d, J = 7.9 Hz, 2H), 2.89–2.67 (m, 4H), 2.44 (ddd, J = 13.7, 6.2, 1.9 Hz, 1H), 2.32–2.15 (m, 1H), 1.79–1.67 (m, 1H), 1.67–1.63 (m, 1H), 1.63–1.49 (m, 2H), 1.49–1.34 (m, 1H). ^{13}C NMR ($CDCl_3$, 75 MHz) δ (ppm): 179.5, 166.5, 152.1, 148.7, 134.7, 123.7, 123.2, 54.6, 47.7, 46.9, 34.4, 30.7, 28.1, 25.1, 21.0.

4.1.6.10. 3-(Pyridin-4-yl)-5-(quinuclidin-3-ylmethyl)-1,2,4-oxadiazole (30).: Applying the general procedure, **62** (392 mg, 1.38 mmol) was treated with CF_3COOH (532 μL, 6.90 mmol) in acetone. After disappearance of the starting material (TLC in cyclohexane/ethyl acetate 1:1), standard workup provided the desired compound **30**. Yellow oil; yield: 340 mg, 91%; R_f = 0.47 (dichloromethane/methanol 95:5, alumina). ^{1}H NMR ($CDCl_3$, 300 MHz) δ (ppm): 8.69 (dd, J = 4.4, 1.7 Hz, 2H), 7.85 (dd, J = 4.5, 1.7 Hz, 2H), 3.20–3.06 (m, 1H), 2.96 (d, J = 7.9 Hz, 2H), 2.86–2.67 (m, 4H), 2.42 (ddd, J = 13.8, 6.2, 1.9 Hz, 1H), 2.28–2.14 (m, 1H), 1.77–1.61 (m, 2H), 1.61–1.48 (m, 2H), 1.48–1.33 (m, 1H). ^{13}C NMR ($CDCl_3$, 75

MHz) δ (ppm): 179.8, 166.9, 150.6, 134.2, 121.2, 54.5, 47.6, 46.8, 34.2, 30.6, 27.9, 24.9, 20.9.

4.1.6.11. 3-(Furan-2-yl)-5-(quinuclidin-3-ylmethyl)-1,2,4-oxadiazole (31).: Applying the general procedure, **63** (158 mg, 0.58 mmol) was treated with CF_3COOH (223 μL, 2.89 mmol) in acetone. After disappearance of the starting material (TLC in cyclohexane/ethyl acetate 7:3), standard workup provided the desired compound **31**. Yellow oil; yield: 146 mg, 97%; R_f = 0.39 (dichloromethane/methanol 85:15, alumina). ^{1}H NMR($CDCl_3$, 300 MHz) δ (ppm): 7.54 (dd, J = 1.7, 0.8 Hz, 1H), 7.05 (dd, J = 3.5, 0.7 Hz, 1H), 6.49 (ddd, J = 3.4, 1.8, 0.7 Hz, 1H), 3.13 (dd, J = 13.0, 10.3 Hz, 1H), 2.93 (d, J = 7.9 Hz, 2H), 2.89–2.67 (m, 4H), 2.43 (dd, J = 13.6, 6.3 Hz, 1H), 2.32–2.14 (m, 1H), 1.80–1.66 (m, 1H), 1.66–1.48 (m, 3H), 1.48–1.34 (m, 1H). ^{13}C NMR ($CDCl_3$, 75 MHz) δ (ppm): 179.0, 161.4, 145.2, 142.4, 113.7, 111.9, 54.5, 47.7, 46.9, 34.3, 30.6, 27.9, 25.0, 20.9.

4.1.6.12. 5-(Quinuclidin-3-ylmethyl)-3-(thiophen-2-yl)-1,2,4-oxadiazole (32).: Applying the general procedure, **64** (336 mg, 1.16 mmol) was treated with CF_3COOH (447 μL, 5.80 mmol) in acetone. After disappearance of the starting material (TLC in cyclohexane/ethyl acetate 3:2 and dichloromethane/methanol 9:1), standard workup provided the desired compound **32**. Yellow oil; yield: 320 mg, 100%; R_f = 0.38 (dichloromethane/methanol 85:15, alumina). ^{1}H NMR ($CDCl_3$, 300MHz) δ (ppm): 7.71 (d, J = 3.7Hz, 1H), 7.42 (d, J = 5.0 Hz, 1H), 7.08 (dd, J = 5.0, 3.7 Hz, 1H), 3.19–3.03 (m, 1H), 2.92 (d, J = 7.8 Hz, 2H), 2.86–2.65 (m, 4H), 2.41 (ddd, J = 13.6, 6.3, 1.8 Hz, 1H), 2.29–2.13 (m, 1H), 1.77–1.47 (m, 4H), 1.47–1.31 (m, 1H). ^{13}C NMR ($CDCl_3$, 75 MHz) δ (ppm): 179.0, 164.5, 129.6, 129.3, 128.5, 128.1, 54.6, 47.8, 46.9, 34.4, 30.7, 28.1, 25.1, 21.0.

4.1.6.13. 3-Phenyl-5-(quinuclidin-3-ylmethyl)-1,2,4-oxadiazole (33).: Applying the general procedure, **65** (370 mg, 1.31 mmol) was reacted with CF_3COOH (503 μL, 6.53 mmol) in acetone. After disappearance of the starting material (TLC in cyclohexane/ethyl acetate 1:1), standard workup provided the desired compound **33**. Yellow oil; yield: 327 mg, 93%; R_f = 0.51 (dichloromethane/methanol 95:5). ^{1}H NMR ($CDCl_3$, 300 MHz) δ (ppm): 8.04–7.95 (m, 2H), 7.47–7.35 (m, 3H), 3.21–3.08 (m, 1H), 2.94 (d, J = 7.9 Hz, 2H), 2.89–2.69 (m, 4H), 2.45 (ddd, J = 13.7, 6.3, 1.9 Hz, 1H), 2.31–2.15 (m, 1H), 1.79–1.63 (m, 2H), 1.63–1.49 (m, 2H), 1.49–1.35 (m, 1H). ^{13}C NMR ($CDCl_3$, 75 MHz) δ (ppm): 178.9, 168.4, 131.2, 128.9, 127.5, 126.9, 54.6, 47.7, 46.9, 34.3, 30.7, 28.0, 25.0, 21.0.

4.1.7. Synthesis of 3-methyl-5-(quinuclidin-3-ylmethyl)-1,2,4-oxadiazole (34)

—Following method B, methyl ester **37** (50 mg, 0.27 mmol) was reacted with acetamidoxime **52** (61 mg, 0.82 mmol) and 60% NaH dispersion in mineral oil (33 mg, 0.82 mmol). After standard extraction, compound **34** was obtained as a pure viscous oil. Light brown oil; yield: 55 mg, 100%; R_f = 0.34 (dichloromethane/methanol 7:3). ^{1}H NMR ($CDCl_3$, 300 MHz) δ (ppm): 3.17–3.01 (m, 1H), 2.84 (d, J = 7.9 Hz, 2H), 2.81–2.65 (m, 4H), 2.37 (ddd, J = 13.7, 6.3, 1.9 Hz, 1H), 2.30 (s, 3H), 2.23–2.07 (m, 1H), 1.73–1.46 (m, 4H), 1.46–1.31 (m, 1H). ^{13}C NMR ($CDCl_3$, 75 MHz) δ (ppm): 178.5, 167.0, 54.5, 47.6, 46.8, 34.1, 30.5, 27.9, 24.9, 20.9, 11.5.

4.1.8. General procedure for the preparation of fumarates (21a-34a)—

A methanol (2 mL/mmol) solution of fumaric acid (1 equiv) was added to a solution of the free base **21**-**34** (1 equiv) in methanol (5 mL/mmol). After stirring at rt for 2 h, additional amounts of fumaric acid (0.5 equiv) were added when no improvement was observed to achieve reaction completion. The crude salts were obtained quantitatively after solvent removal and then recrystallized to give the desired final compounds **21a**-**34a** as crystalline derivatives.

4.1.8.1. 3-(3-Fluorophenyl)-5-(quinuclidin-3-ylmethyl)-1,2,4-oxadiazole fumarate (21a).: The free base **21** (220 mg, 0.77 mmol) and fumaric acid (89 mg, 0.77 mmol) were reacted in methanol. The crude salt was recrystallized from ethyl acetate/*n*-hexane to provide the pure compound **21a** (**21** × $C_4H_4O_4$). Colorless solid; yield: 89 mg, 29%; mp 158–160 °C. ^{1}H NMR (CD_3OD, 300 MHz) δ (ppm): 7.92–7.85 (m, 1H), 7.76 (ddd, J = 9.6, 2.6, 1.5 Hz, 1H), 7.55 (td, J = 8.0, 5.7 Hz, 1H), 7.30 (tdd, J = 8.5, 2.7, 1.0 Hz, 1H), 6.68 (s, 2H), 3.72 (ddd, J = 12.8,10.2, 2.4 Hz, 1H), 3.46–3.17 (m, 6H), 3.12 (ddd, J = 13.0, 7.1, 1.8 Hz, 1H), 2.89–2.72 (m, 1H), 2.26–2.09 (m, 2H), 2.09–1.99 (m, 2H), 1.99–1.84 (m, 1H). ^{13}C NMR (CD_3OD, 75 MHz) δ (ppm): 179.9, 171.4, 168.6, 164.3 (d, J = 245.4 Hz), 136.2, 132.2 (d, J = 8.2 Hz), 130.2 (d, J = 8.5 Hz), 124.2 (d, J = 3.1 Hz), 119.3 (d, J = 21.5 Hz), 115.0 (d, J = 24.1 Hz), 53.0, 47.5, 47.0, 32.6, 30.1, 25.3, 24.9, 19.0. MS (ESI) *m/z* calcd. for $C_{16}H_{19}FN_3O^+$ $[M+H]^+$: 288.2; found: 288.0.

4.1.8.2. 3-(3-Chlorophenyl)-5-(quinuclidin-3-ylmethyl)-1,2,4-oxadiazole fumarate (22a).: The free base **22** (250 mg, 0.82 mmol) and fumaric acid (96 mg, 0.82 mmol) were reacted in methanol. The crude salt was recrystallized from absolute ethanol/acetone to provide the pure compound **22a** (**22** × 0.75$C_4H_4O_4$). Colorless solid; yield: 153 mg, 48%; mp 152–154°C. ^{1}H NMR (CD_3OD, 300 MHz) δ (ppm): 8.04 (m, 1H), 7.98 (dt, J = 7.2, 1.5 Hz, 1H), 7.59–7.54 (m, 1H), 7.54–7.47 (m, 1H), 6.67 (s, 1.5H), 3.72 (ddd, J = 12.8, 10.2, 2.4 Hz, 1H), 3.46–3.17 (m, 6H), 3.11 (ddd, J = 13.1, 7.1, 1.6 Hz, 1H), 2.88–2.72 (m, 1H), 2.27–2.09 (m, 2H), 2.09–1.99 (m, 2H), 1.99–1.85 (m, 1H). ^{13}C NMR (CD_3OD, 75 MHz) δ (ppm): 179.9, 171.5, 168.5, 136.2, 136.0, 132.4, 131.8, 129.9, 128.2, 126.6, 53.0, 47.6, 47.0, 32.6, 30.1, 25.3, 25.0, 19.0. MS (ESI) *m/z* calcd. for $C_{16}H_{19}ClN_3O^+$ $[M+H]^+$: 304.1; found: 304.1.

4.1.8.3. 3-(3-Bromophenyl)-5-(quinuclidin-3-ylmethyl)-1,2,4-oxadiazole fumarate (23a).: The free base **23** (200 mg, 0.57 mmol) and fumaric acid (67 mg, 0.57 mmol) were reacted in methanol. The crude salt was recrystallized from absolute ethanol/acetone to provide the pure compound **23a** (**23** × 0.75$C_4H_4O_4$). Colorless solid; yield: 137 mg, 55%; mp 142–144 °C. ^{1}H NMR (CD_3OD, 300 MHz) δ (ppm): 8.19 (t, J = 1.8 Hz, 1H), 8.03 (dt, J = 7.8, 1.2 Hz, 1H), 7.71 (ddd, J = 8.0, 1.9, 1.0 Hz, 1H), 7.44 (t, J = 7.9 Hz, 1H), 6.67 (s, 1.5H), 3.72 (ddd, J = 12.8, 10.2, 2.4 Hz, 1H), 3.45–3.17 (m, 6H), 3.11 (ddd, J = 13.0, 7.0, 1.6 Hz, 1H), 2.88–2.71 (m, 1H), 2.26–2.10 (m, 2H), 2.10–1.99 (m, 2H), 1.99–1.85 (m, 1H). ^{13}C NMR (CD_3OD, 75 MHz) δ (ppm): 180.0, 171.5, 168.4, 136.2, 135.4, 132.0, 131.1, 130.1, 127.0, 123.9, 53.0, 47.6, 47.1, 32.6, 30.1, 25.3, 24.9, 19.0. MS (ESI) *m/z* calcd. for $C_{16}H_{19}BrN_3O^+$ $[M+H]^+$: 348.1; found: 348.3.

4.1.8.4. 3-(3-Iodophenyl)-5-(quinuclidin-3-ylmethyl)-1,2,4-oxadiazole fumarate (24a).: The free base **24** (294 mg, 0.74 mmol) and fumaric acid (86 mg, 0.74 mmol) were reacted in methanol. The crude salt was recrystallized from methanol/*n*-hexane to provide the pure compound **24a** (**24** × $C_4H_4O_4$). Colorless solid; yield: 321 mg, 85%; mp 154–156 °C. ^{1}H NMR (CD_3OD, 300 MHz) δ (ppm): 8.38 (t, J = 1.7 Hz, 1H), 8.07–8.01 (m, 1H), 7.93–7.87 (m, 1H), 7.29 (t, J = 7.9 Hz, 1H), 6.69 (s, 2H), 3.72 (ddd, J = 12.8, 10.2, 2.4Hz, 1H), 3.45–3.16 (m, 6H), 3.11 (ddd, J = 13.1, 7.0, 1.7 Hz, 1H), 2.88–2.72 (m, 1H), 2.26–2.09 (m, 2H), 2.09–1.98 (m, 2H), 1.98–1.84 (m, 1H). ^{13}C NMR (CD_3OD, 75 MHz) δ (ppm): 179.9, 169.9, 168.2, 141.4, 137.1, 135.7, 131.9, 129.9, 127.5, 95.0, 52.9, 47.5, 47.0, 32.6, 30.1, 25.3, 24.9, 19.0. MS (ESI) *m/z* calcd. for $C_{16}H_{19}IN_3O^+$ $[M+H]^+$: 396.1; found: 396.0.

4.1.8.5. 5-(Quinuclidin-3-ylmethyl)-3-(3-(trifluoromethyl)phenyl)-1,2,4-oxadiazole fumarate (25a).: The free base **25** (180 mg, 0.53 mmol) and fumaric acid (62 mg, 0.53 mmol) were reacted in methanol. After 2 h, additional fumaric acid (31 mg, 0.27 mmol) was added. The crude salt was recrystallized from ethyl acetate/*n*-hexane to provide the pure compound **25a** (**25** × 1.5$C_4H_4O_4$). Colorless solid; yield: 111 mg, 41%; mp 129–130°C. ^{1}H NMR (CD_3OD, 300 MHz) δ (ppm): 8.30–8.19 (m, 2H), 7.84–7.74 (m, 1H), 7.73–7.61 (m, 1H), 6.63 (s, 3H), 3.75–3.58 (m, 1H), 3.40–3.11 (m, 6H), 3.11–2.98 (m, 1H), 2.85–2.66 (m, 1H), 2.07 (s, 2H), 1.98 (s, 2H), 1.87 (s, 1H). ^{13}C NMR (CD_3OD, 75 MHz) δ (ppm): 180.2, 170.0, 168.5, 135.8, 132.5 (q, J = 32.8 Hz), 131.8, 131.2, 129.1, 129.0 (q, J = 3.6 Hz), 125.3 (q, J = 271.6 Hz), 124.9 (q, J = 3.9 Hz), 53.0, 47.6, 47.1, 32.6, 30.1, 25.3, 24.9, 19.0. MS (ESI) *m/z* calcd. for $C_{17}H_{19}F_3N_3O^+$ $[M+H]^+$: 338.2; Found: 338.1.

4.1.8.6. 5-(Quinuclidin-3-ylmethyl)-3-(m-tolyl)-1,2,4-oxadiazole fumarate (26a).: The free base **26** (68 mg, 0.24 mmol) and fumaric acid (28 mg, 0.24 mmol) were reacted in methanol. After 2 h, additional fumaric acid (14 mg, 0.12 mmol) was added twice. The crude salt was recrystallized from acetone to provide the pure compound **26a** (**26** × 2$C_4H_4O_4$). Colorless solid; yield: 109 mg, 88%; mp 210–215 °C (dec.). ^{1}H NMR (CD_3OD, 300 MHz) δ (ppm): 7.91–7.86 (m, 1H), 7.86–7.80 (m, 1H), 7.44–7.34 (m, 2H), 6.76 (s, 4H), 3.74 (ddd, J = 12.8, 10.2, 2.5 Hz, 1H), 3.48–3.33 (m, 4H), 3.25 (dd, J = 7.7, 5.7 Hz, 2H), 3.14 (ddd, J = 13.0, 7.1, 1.8 Hz, 1H), 2.89–2.74 (m, 1H), 2.42 (s, 3H), 2.28–2.11 (m, 2H), 2.11–2.01 (m, 2H), 2.01–1.85 (m, 1H). ^{13}C NMR (CD_3OD, 75 MHz) δ (ppm): 179.4, 169.6, 168.1, 140.1, 135.2, 133.2, 130.0, 128.8, 127.8, 125.5, 53.1, 47.7, 47.2, 32.6, 30.1, 25.2, 24.9, 21.4, 18.9. MS (ESI) *m/z* calcd. for $C_{17}H_{22}N_3O^+$ $[M+H]^+$: 284.2; found: 284.4.

4.1.8.7. 3-(3-Methoxyphenyl)-5-(quinuclidin-3-ylmethyl)-1,2,4-oxadiazole fumarate (27a).: The free base **27** (375 mg, 1.25 mmol) and fumaric acid (145 mg, 1.25 mmol) were reacted in methanol. The crude salt was recrystallized from methanol/*n*-hexane to provide the pure compound **27a** (**27** × 1.5$C_4H_4O_4$). Colorless solid; yield: 140 mg, 24%; mp 148–149 °C. ^{1}H NMR (CD_3OD, 300 MHz) δ (ppm): 7.62 (dt, J = 7.7, 1.1 Hz 1H), 7.57 (dd, J = 2.6, 1.5 Hz, 1H), 7.42 (t, J = 8.0 Hz, 1H), 7.10 (ddd, J = 8.3, 2.6, 0.9 Hz, 1H), 6.68 (s, 1.5H), 3.85 (s, 3H), 3.71 (ddd, J = 12.8, 10.2, 2.4 Hz, 1H), 3.45–3.28 (m, 4H), 3.24 (dd, J = 7.7, 6.5 Hz, 2H), 3.11 (ddd, J = 13.0, 7.0, 1.6 Hz, 1H), 2.87–2.72 (m,1H), 2.25–2.09 (m, 2H), 2.09–1.98 (m, 2H), 1.98–1.84 (m, 1H). ^{13}C NMR (CD_3OD, 75 MHz) δ (ppm): 179.5, 171.4,

169.5, 161.5, 136.2, 131.2, 129.1, 120.6, 118.2, 113.5, 55.9, 53.0, 47.6, 47.1, 32.7, 30.1, 25.3, 24.9, 19.0. MS (ESI) *m/z* calcd. for $C_{17}H_{22}N_3O_2^+$ $[M+H]^+$: 300.2; found: 300.0.

4.1.8.8. 3-(4-Methoxyphenyl)-5-(quinuclidin-3-ylmethyl)-1,2,4-oxadiazole fumarate (28a).: The free base **28** (57 mg, 0.19 mmol) and fumaric acid (22 mg, 0.19 mmol) were reacted in methanol. After 2 h, additional fumaric acid (11 mg, 0.10 mmol) was added. The crude salt was recrystallized from methanol/*n*-hexane to provide the pure compound **28a** (**28** × $1.25C_4H_4O_4$). Colorless solid; yield: 25 mg, 30%; mp 175–176 °C. ^{1}H NMR (CD_3OD, 300 MHz) δ (ppm): 7.97 (d, J = 9.0 Hz, 2H), 7.04 (d, J = 9.0 Hz, 2H), 6.69 (s, 2.5H), 3.86 (s, 3H), 3.77–3.64 (m, 1H), 3.46–3.26 (m, 4H), 3.22 (dd, J = 7.7, 5.5 Hz, 2H), 3.18–3.05 (m, 1H), 2.87–2.71 (m, 1H), 2.27–2.09 (m, 2H), 2.09–1.99 (m, 2H), 1.99–1.84 (m, 1H). ^{13}C NMR (CD3OD, 75 MHz) δ (ppm): 179.2, 170.6, 169.3, 163.8, 136.0, 130.0, 120.2, 115.4, 56.0, 53.1, 47.7, 47.1, 32.7, 30.1, 25.2, 24.9, 19.0. MS (ESI) *m/z* calcd. for $C_{17}H_{22}N_3O_2^+$ $[M+H]^+$: 300.2; found: 300.0.

4.1.8.9. 3-(Pyridine-3-yl)-5-(quinuclidin-3-ylmethyl)-1,2,4-oxadiazole fumarate (29a).: The free base **29** (225 mg, 0.83 mmol) and fumaric acid (97 mg, 0.83 mmol) were reacted in methanol. After 2 h, additional fumaric acid (48 mg, 0.42 mmol) was added. The crude salt was recrystallized from methanol/propan-2-ol to provide the pure compound **29a** (**29** × $1.25C_4H_4O_4$). Colorless solid; yield: 185 mg, 54%; mp 182–183 °C. ^{1}H NMR (CD_3OD, 300 MHz) δ (ppm): 9.20 (d, J = 1.5Hz, 1H), 8.72 (dd, J = 4.9, 1.5Hz, 1H), 8.51–8.42 (m, 1H), 7.61 (ddd, J = 8.0, 5.0, 0.8 Hz, 1H), 6.71 (s, 2.5H), 3.74 (ddd, J = 12.8, 10.2, 2.4 Hz, 1H), 3.47–3.32 (m, 4H), 3.29 (dd, J = 5.2, 2.8 Hz, 2H), 3.14 (ddd, J = 13.1, 7.0, 1.9 Hz, 1H), 2.91 −2.74 (m, 1H), 2.31–2.11 (m, 2H), 2.11–2.00 (m, 2H), 2.00–1.85 (m, 1H). ^{13}C NMR (CD_3OD, 75 MHz) δ (ppm): 180.3, 169.9, 167.5, 152.7, 148.8, 136.6, 135.7, 125.7, 124.9, 53.0, 47.6, 47.1, 32.6, 30.1, 25.3, 24.9, 19.0. MS (ESI) *m/z* calcd. for $C_{15}H_{19}N_4O^+$ $[M+H]^+$: 271.2; found: 271.4.

4.1.8.10. 3-(Pyridin-4-yl)-5-(quinuclidin-3-ylmethyl)-1,2,4-oxadiazole fumarate (30a).: The free base **30** (340 mg, 1.26 mmol) and fumaric acid (146 mg, 1.26 mmol) were reacted in methanol. After 2 h, additional fumaric acid (73 mg, 0.63 mmol) was added. The crude salt was recrystallized from methanol/absolute ethanol to provide the pure compound **30a** (**30** × 1.5C4H4O4). Colorless solid; yield: 168 mg, 30%; mp 188–190°C. ^{1}H NMR (CD_3OD, 300 MHz) δ (ppm): 8.74 (dd, J = 4.7, 1.5 Hz, 2H), 8.04 (dd, J = 4.6, 1.6Hz, 2H), 6.71 (s, 3H), 3.73 (ddd, J = 12.8, 10.2, 2.4Hz, 1H), 3.46–3.19 (m, 6H), 3.12 (ddd, J = 13.0, 7.0, 1.8 Hz, 1H), 2.89–2.73 (m, 1H), 2.26–2.10 (m, 2H), 2.10–1.99 (m, 2H), 1.99–1.84 (m, 1H). ^{13}C NMR (CD_3OD, 75 MHz) δ (ppm): 180.6, 169.9, 167.9, 151.3, 136.4, 135.7, 122.8, 52.9, 47.5, 47.0, 32.6, 30.1, 25.3, 24.9, 19.0. MS (ESI) *m/z* calcd. for $C_{15}H_{19}N_4O^+$ $[M+H]^+$: 271.2; found: 271.4.

4.1.8.11. 3-(Furan-2-yl)-5-(quinuclidin-3-ylmethyl)-1,2,4-oxadiazole fumarate (31a).: The free base **31** (78 mg, 0.30 mmol) and fumaric acid (35 mg, 0.30 mmol) were reacted in methanol. The crude salt was recrystallized from methanol/*n*-hexane to provide the pure compound **31a** (**31** × $C_4H_4O_4$). Colorless solid; yield: 93 mg, 83%; mp 158–159 °C. ^{1}H NMR (CD_3OD, 300 MHz) δ (ppm): 7.75 (dd, J = 1.8, 0.8 Hz, 1H), 7.15 (dd, J =

3.5, 0.6 Hz, 1H), 6.68 (s, 2H), 6.65 (dd, *J* = 3.5, 1.8 Hz, 1H), 3.69 (ddd, *J* = 12.8, 10.2, 2.3 Hz, 1H), 3.45–3.27 (m, 4H), 3.23 (dd, *J* = 7.7, 5.1 Hz, 2H), 3.09 (ddd, *J* = 13.0, 7.0, 1.8 Hz, 1H), 2.87–2.69 (m, 1H), 2.25–2.08 (m, 2H), 2.08–1.98 (m, 2H), 1.98–1.82 (m, 1H). ^{13}C NMR (CD_3OD, 75 MHz) δ (ppm): 179.5, 171.3, 162.4, 147.0, 143.5, 136.2, 115.1, 113.0, 52.9, 47.6, 47.1, 32.6, 30.0, 25.2, 24.9, 18.9. MS (ESI) *m/z* calcd. for $C_{14}H_{18}N_3O_2^+$ $[M+H]^+$: 260.1; found: 260.0.

4.1.8.12. 5-(Quinuclidin-3-ylmethyl)-3-(thiophen-2-yl)-1,2,4-oxadiazole fumarate (32a).: The free base **32** (320 mg, 1.16 mmol) and fumaric acid (135 mg, 1.16 mmol) were reacted in methanol. The crude salt was recrystallized from acetone to provide the pure compound **32a** (**32** × $0.75C_4H_4O_4$). Colorless solid; yield: 303 mg, 72%; mp 145–147 °C. ^{1}H NMR (CD_3OD, 300 MHz) δ (ppm): 7.79 (dd, *J* = 3.6, 1.2 Hz, 1H), 7.68 (dd, *J* = 5.0, 1.1 Hz, 1H), 7.20 (dd, *J* = 5.0, 3.7 Hz, 1H), 6.68 (s, 1.5H), 3.70 (ddd, *J* = 12.8, 10.2, 2.4 Hz, 1H), 3.46–3.27 (m, 4H), 3.23 (dd, *J* = 7.7, 5.8 Hz, 2H), 3.11 (ddd, *J* = 13.0, 7.0, 1.7 Hz, 1H), 2.86–2.71 (m, 1H), 2.27–2.09 (m, 2H), 2.09–1.99 (m, 2H), 1.99–1.85 (m, 1H). ^{13}C NMR (CD_3OD, 75 MHz) δ (ppm): 179.5, 171.4, 165.7, 136.2, 130.9, 130.8, 129.2, 129.1, 53.0, 47.6, 47.1, 32.6, 30.0, 25.3, 24.9,19.0. MS (ESI) *m/z* calcd. for $C_{14}H_{18}N_3OS^+$ $[M+H]^+$: 276.1; found: 276.6.

4.1.8.13. 3-Phenyl-5-(quinuclidin-3-ylmethyl)-1,2,4-oxadiazole fumarate (33a).: The free base **33** (327 mg, 1.21 mmol) and fumaric acid (141 mg, 1.21 mmol) were reacted in methanol. The crude salt was recrystallized from methanol/diethyl ether to provide the pure compound **33a** (**33** × $C_4H_4O_4$). Colorless solid; yield: 308 mg, 66%; mp 142–143 °C. ^{1}H NMR(CD_3OD, 300 MHz) δ (ppm): 8.08–8.01 (m, 2H), 7.58–7.46 (m, 3H), 6.68 (s, 2H), 3.71 (ddd, *J* = 12.8, 10.2, 2.4 Hz, 1H), 3.43–3.16 (m, 6H), 3.11 (ddd, *J* = 13.1, 7.0,1.9 Hz, 1H), 2.86–2.72 (m, 1H), 2.25–2.09 (m, 2H), 2.09–1.98 (m, 2H), 1.98–1.84 (m, 1H). ^{13}C NMR (CD_3OD, 75 MHz) δ (ppm): 179.6, 171.4, 169.5, 136.2, 132.5, 130.1, 128.3, 128.0, 53.0, 47.5, 47.0, 32.7, 30.1, 25.3, 24.9, 19.0. MS (ESI) *m/z* calcd. for $C_{16}H_{20}N_3O^+$ $[M+H]^+$: 270.2; found: 270.5.

4.1.8.14. 3-Methyl-5-(quinuclidin-3-ylmethyl)-1,2,4-oxadiazole fumarate (34a).: The free base **34** (55 mg, 0.27 mmol) and fumaric acid (31 mg, 0.27 mmol) were reacted in methanol. After 2 h, additional fumaric acid (16 mg, 0.14 mmol) was added. The crude salt was recrystallized from propan-2-ol to provide the pure compound **34a** (**34** × $1.25C_4H_4O_4$). Colorless solid; yield: 76 mg, 80%; mp 158–159 °C. ^{1}H NMR (CD_3OD, 300 MHz) δ (ppm): 6.70 (s, 2.5H), 3.64 (ddd, *J* = 12.8, 10.2, 2.4 Hz, 1H), 3.43–3.18 (m, 4H), 3.14 (dd, *J* = 7.7, 4.4 Hz, 2H), 3.04 (ddd, *J* = 13.0, 7.0, 2.0 Hz, 1H), 2.77–2.62 (m, 1H), 2.34 (s, 3H), 2.22–2.10 (m, 1H), 2.10–1.96 (m, 3H), 1.96–1.82 (m, 1H). ^{13}C NMR (CD_3OD, 75 MHz) δ (ppm): 179.1, 170.6, 168.5, 136.0, 52.9, 47.5, 47.0, 32.6, 29.9, 25.1, 24.9, 18.9, 11.3. MS (ESI) *m/z* calcd. for $C_{11}H_{18}N_3O^+$ $[M+H]^+$: 208.1; found: 208.2.

4.1.9. General procedure for the preparation of quaternary salts (21b-34b)—

Methyl iodide (8 equiv) was added to a solution of the free base **21**-**34** (1 equiv) in methanol (5 mL/mmol). After stirring overnight at rt, the mixture was evaporated under reduced pressure to provide the crude *N*-methylated analogs **21b**-**34b**, which were recrystallized.

4.1.9.1. 3-(3-Fluorophenyl)-5-(quinuclidin-3-ylmethyl)-1,2,4-oxadiazole methiodide (21b).: CH_3I (433 μL, 6.96 mmol) was added to a solution of the free base **21** (250 mg, 0.87 mmol) in methanol. After evaporation of the solvent, the crude quaternary salt was recrystallized from methanol/absolute ethanol to give the pure compound **21b** (**21** × CH_3I). Colorless solid; yield: 128 mg, 34%; mp 150–151 °C. ^{1}H NMR(CD_3OD, 300 MHz) δ (ppm): 7.92–7.86 (m,1H), 7.80–7.74 (m, 1H), 7.55 (td, J = 8.0, 5.9 Hz, 1H), 7.35–7.26 (m, 1H), 3.94–3.82 (m, 1H), 3.59–3.46 (m, 4H), 3.40–3.19 (m, 3H), 3.02 (s, 3H), 2.99–2.83 (m, 1H), 2.34–2.17 (m, 2H), 2.17–2.07 (m, 2H), 2.07–1.92 (m, 1H). ^{13}C NMR (CD_3OD, 75 MHz) δ (ppm): 179.7, 168.7, 164.3 (d, J = 245.4 Hz), 132.2 (d, J = 8.4 Hz), 130.1 (d, J = 8.4 Hz), 124.3 (d, J = 3.2 Hz), 119.3 (d, J = 21.5 Hz), 115.1 (d, J = 24.1 Hz), 63.0, 58.0, 57.6, 52.6, 33.6, 30.1, 25.9, 25.2, 20.3. MS (ESI) m/z calcd. for $C_{17}H_{21}FN_3O^+$ $[M]^+$: 302.2; found 302.0.

4.1.9.2. 3-(3-Chlorophenyl)-5-(quinuclidin-3yl-methyl)-1,2,4-oxadiazole methiodide (22b).: CH_3I (466 μL, 7.48 mmol) was added to a solution of the free base **22** (284 mg, 0.94 mmol) in methanol. After evaporation of the solvent, the crude quaternary salt was recrystallized from methanol/absolute ethanol to give the pure compound **22b** (**22** × CH_3I). Colorless solid; yield: 194 mg, 47%; mp 119–120°C. ^{1}H NMR (CD_3OD, 300 MHz) δ (ppm): 8.06–8.03 (m, 1H), 8.02–7.97 (m, 1H), 7.59–7.54 (m, 1H), 7.54–7.47 (m, 1H), 3.95–3.81 (m, 1H), 3.61–3.46 (m, 4H), 3.42–3.19 (m, 3H), 3.03 (s, 3H), 2.98–2.84 (m, 1H), 2.36–2.17 (m, 2H), 2.17–2.08 (m, 2H), 2.8–1.92 (m,1H). ^{13}C NMR (CD_3OD, 75 MHz) δ (ppm): 179.7, 168.5, 136.0, 132.4, 131.8, 129.9, 128.2, 126.7, 63.0, 58.0, 57.6, 52.7, 33.6, 30.2, 25.9, 25.2, 20.3. MS (ESI) m/z calcd. for $C_{17}H_{21}ClN_3O^+$ $[M]^+$: 318.1; found: 318.2.

4.1.9.3. 3-(3-Bromophenyl)-5-(quinuclidin-3-ylmethyl)-1,2,4-oxadiazole methiodide (23b).: CH_3I (286 μL, 4.59 mmol) was added to a solution of the free base **23** (200 mg, 0.57 mmol) in methanol. After evaporation of the solvent, the crude quaternary salt was recrystallized from absolute ethanol/acetone to give the pure compound **23b** (**23** × CH_3I). Colorless solid; yield: 160 mg, 57%; mp 171–173 °C (dec.). ^{1}H NMR (CD_3OD, 300 MHz) δ (ppm): 8.19 (t, J = 1.7 Hz, 1H), 8.06–8.01 (m, 1H), 7.71 (ddd, J = 8.1, 2.0, 1.0 Hz, 1H), 7.45 (t, J = 7.9 Hz, 1H), 3.94–3.81 (m, 1H), 3.59–3.47 (m, 4H), 3.42–3.19 (m, 3H), 3.03 (s, 3H), 3.00–2.83 (m, 1H), 2.34–2.18 (m, 2H), 2.18–2.08 (m, 2H), 2.08–1.92 (m, 1H). ^{13}C NMR (CD3OD, 75 MHz) δ (ppm): 179.7, 168.4, 135.4, 132.0, 131.1, 130.1, 127.1, 123.8, 63.0, 58.0, 57.6, 52.7, 33.6, 30.2, 25.9, 25.2, 20.3. MS (ESI) m/z calcd. for $C_{17}H_{21}BrN_3O^+$ $[M]^+$: 362.1; found: 362.3.

4.1.9.4. 3-(3-Iodophenyl)-5-(quinuclidin-3-ylmethyl)-1,2,4-oxadiazole methiodide (24b).: CH_3I (344 μL, 5.52 mmol) was added to a solution of the free base **24** (271 mg, 0.69 mmol) in methanol to give the pure compound **24b** (**24** × CH_3I). After evaporation of the solvent, the crude quaternary salt was recrystallized from methanol. Bright colorless crystals; yield: 167 mg, 45%; mp 234–236 °C (dec.). ^{1}H NMR (CD_3OD, 300 MHz) δ (ppm): 8.39 (t, J = 1.6 Hz, 1H), 8.9–8.03 (m, 1H), 7.91 (ddd, J = 7.9, 1.8, 1.1 Hz, 1H), 7.29 (t, J = 7.9 Hz, 1H), 3.95–3.76 (m, 1H), 3.58–3.42 (m, 4H), 3.40–3.15 (m, 3H), 3.01 (s, 3H), 2.97–2.82 (m, 1H), 2.35–2.18 (m, 2H), 2.18–2.08 (m, 2H), 2.08–1.92 (m, 1H). ^{13}C NMR (CD_3OD, 75 MHz) δ (ppm): 179.7, 168.3, 141.5, 137.1, 131.9, 129.9, 127.5, 95.0, 63.1,

58.0, 57.6, 52.7, 33.6, 30.2, 25.9, 25.2, 20.3. MS (ESI) *m/z* calcd. for $C_{17}H_{21}IN_3O^+$ $[M]^+$: 410.1; found: 410.3.

4.1.9.5. 5-(Quinuclidin-3-ylmethyl)-3-(3-(trifluoromethyl)phenyl)-1,2,4-oxadiazole methiodide (25b).: CH_3I (224 μL, 3.60 mmol) was added to a solution of the free base **25** (150 mg, 0.45 mmol) in methanol. After evaporation of the solvent, the crude quaternary salt was recrystallized from methanol/absolute ethanol to give the pure compound **25b** (**25** × CH_3I). Colorless solid; yield: 147 mg, *68%*; mp 170–172 °C (dec.). ^1H NMR (CD_3OD, 300 MHz) δ (ppm): 8.37–8.29 (m, 2H), 7.90–7.83 (m, 1H), 7.79–7.70 (m, 1H), 3.95–3.81 (m, 1H), 3.61–3.47 (m, 4H), 3.42–3.21 (m, 3H), 3.03 (s, 3H), 3.00–2.85 (m, 1H), 2.35–2.18 (m, 2H), 2.18–2.09 (m, 2H), 2.09–1.93 (m, 1H). ^{13}C NMR (CD_3OD, 75 MHz) δ (ppm): 180.0, 168.5, 132.5 (q, J = 32.7 Hz), 131.9, 131.2, 129.1, 129.0 (q, J = 3.8 Hz), 125.3 (q, J = 271.5 Hz), 124.9 (q, J = 3.9 Hz), 63.0, 58.0, 57.6, 52.7, 33.6, 30.2, 25.9, 25.2, 20.3. MS (ESI) *m/z* calcd. for $C_{18}H_{21}F_3N_3O^+$ $[M]^+$: 352.2; found: 352.4.

4.1.9.6. 5-(Quinuclidin-3-ylmethyl)-3-(m-tolyl)-1,2,4-oxadiazole methiodide (26b).: CH_3I (557 μL, 8.95 mmol) was added to a solution of the free base **26** (317 mg, 1.12 mmol) in methanol. After evaporation of the solvent, the crude quaternary salt was recrystallized from methanol/absolute ethanol to give the pure compound **26b** (**26** × CH_3I). Colorless solid; yield: 191 mg, 40%; mp 162–164 °C. ^1H NMR (CD_3OD, 300 MHz) δ (ppm): 7.90–7.81 (m, 2H), 7.42–7.33 (m, 2H), 3.95–3.82 (m, 1H), 3.60–3.49 (m, 4H), 3.41–3.18 (m, 3H), 3.03 (s, 3H), 3.00–2.83 (m, 1H), 2.41 (s, 3H), 2.35–2.22 (m, 1H), 2.22–2.17 (m, 1H), 2.17–2.08 (m, 2H), 2.08–1.95 (m, 1H). ^{13}C NMR (CD_3OD, 75 MHz) δ (ppm): 179.2, 169.6, 140.1, 133.2, 130.0, 128.8, 127.8, 125.5, 63.1, 58.0, 57.6, 52.6, 33.6, 30.2, 25.9, 25.2, 21.4, 20.3. MS (ESI) *m/z* calcd. for $C_{18}H_{24}N_3O^+$ $[M]^+$: 298.2; found: 298.1.

4.1.9.7. 3-(3-Methoxyphenyl)-5-(quinuclidin-3-ylmethyl)-1,2,4-oxadiazole methiodide (27b).: CH_3I (237 μL, 3.47 mmol) was added to a solution of the free base **27** (130 mg, 0.43 mmol) in methanol. After evaporation of the solvent, the crude quaternary salt was recrystallized from methanol/absolute ethanol/diethyl ether to give the pure compound **27b** (**27** × CH_3I). Yellowish solid; yield: 76 mg, 40%; mp 178–179 °C. ^1H NMR (CD_3OD, 300 MHz) δ (ppm): 7.67–7.60 (m, 1H), 7.60–7.55 (m, 1H), 7.42 (t, J = 8.0 Hz, 1H), 7.11 (dd, J = 8.3, 2.2 Hz, 1H), 3.93–3.79 (m, 4H), 3.52 (t, J = 7.9 Hz, 4H), 3.40–3.17 (m, 3H), 3.02 (s, 3H), 2.98–2.82 (m, 1H), 2.35–2.17 (m, 2H), 2.17–2.08 (m, 2H), 2.08–1.93 (m, 1H). ^{13}C NMR (CD_3OD, 75 MHz) δ (ppm): 179.3, 169.5, 161.5, 131.3, 129.1, 120.6, 118.2, 113.6, 63.0, 58.0, 57.5, 55.9, 52.6, 33.6, 30.1, 25.9, 25.2, 20.3. MS (ESI) *m/z* calcd. for $C_{18}H_{24}N_3O_2^+$ $[M]^+$: 314.2; found: 314.2.

4.1.9.8. 3-(4-Methoxyphenyl)-5-(quinuclidin-3-ylmethyl)-1,2,4-oxadiazole methiodide (28b).: CH_3I (135 μL, 1.98 mmol) was added to a solution of the free base **28** (74 mg, 0.25 mmol) in methanol. After evaporation of the solvent, the crude quaternary salt was recrystallized from methanol/absolute ethanol to give the pure compound **28b** (**28** × CH_3I). Colorless solid; yield: 70 mg, 63%; mp 192–193 °C (dec.). ^1H NMR (CD_3OD, 300 MHz) δ (ppm): 7.98 (d, J = 9.0 Hz, 2H), 7.04 (d, J = 9.0 Hz, 2H), 3.93–3.77 (m, 4H), 3.52 (t, J = 7.9 Hz, 4H), 3.39–3.13 (m, 3H), 3.01 (s, 3H), 2.97–2.80 (m, 1H), 2.35–2.17 (m, 2H), 2.17–2.08

(m, 2H), 2.08–1.91 (m, 1H). ^{13}C (CD_3OD, 75 MHz) δ (ppm): 179.0, 169.3, 163.8, 130.0, 120.1, 115.4, 63.1, 58.0, 57.6, 56.0, 52.6, 33.7, 30.1, 25.9, 25.2, 20.3. MS (ESI) *m/z* calcd. for $C_{18}H_{24}N_3O_2^+$ $[M]^+$: 314.2; found: 314.2.

4.1.9.9. 3-(Pyridine-3-yl)-5-(quinuclidin-3-ylmethyl)-1,2,4-oxadiazole methiodide (29b).: CH_3I (232 μL, 3.73 mmol) was added to a solution of the free base **29** (126 mg, 0.47 mmol) in methanol. After evaporation of the solvent, the crude quaternary salt was recrystallized from methanol/absolute ethanol to give the pure compound **29b** (**29** × CH_3I). Colorless solid; yield: 55 mg, 28%; mp 140–142 °C. ^{1}H NMR(CD_3OD, 300 MHz) δ (ppm): 9.20 (dd, *J* = 2.0, 0.7 Hz, 1H), 8.72 (dd, *J* = 4.9, 1.6 Hz, 1H), 8.48 (dt, *J* = 8.0, 1.9 Hz, 1H), 7.64–7.57 (m, 1H), 3.95–3.82 (m, 1H), 3.60–3.46 (m, 4H), 3.43–3.21 (m, 3H), 3.03 (s, 3H), 2.99–2.84 (m, 1H), 2.34–2.19 (m, 2H), 2.19–2.08 (m, 2H), 2.08–1.94 (m, 1H). ^{13}C NMR (CD_3OD, 75 MHz) δ (ppm): 180.1, 167.4, 152.7, 148.8, 136.6, 125.7, 124.9, 63.0, 58.0, 57.6, 52.7, 33.6, 30.13, 25.9, 25.2, 20.3. MS (ESI) *m/z* calcd. for $C_{16}H_{21}N_4O^+$ $[M]^+$: 285.2; found: 285.0.

4.1.9.10. 3-(Pyridine-4-yl)-5-(quinuclidin-3-ylmethyl)-1,2,4-oxadiazole methiodide (30b).: CH_3I (475 μL, 7.64 mmol) was added to a solution of the free base **30** (258 mg, 0.95 mmol) in methanol. After evaporation of the solvent, the crude quaternary salt was recrystallized from methanol/absolute ethanol to give the pure compound **30b** (**30** × CH_3I). Yellowish solid; yield: 143 mg, 37%; mp 152–155 °C. ^{1}H NMR (CD_3OD, 300 MHz) δ (ppm): 8.77–8.71 (m, 2H), 8.10–8.02 (m, 2H), 3.97–3.84 (m, 1H), 3.62–3.47 (m, 4H), 3.44–3.23 (m, 3H), 3.04 (s, 3H), 3.00–2.84 (m, 1H), 2.35–2.19 (m, 2H), 2.19–2.09 (m, 2H), 2.09–1.92 (m, 1H). ^{13}C NMR (CD_3OD, 75 MHz) δ (ppm): 180.4, 167.9, 151.3, 136.4, 122.8, 63.0, 58.0, 57.6, 52.7, 33.6, 30.1, 25.9, 25.2, 20.3. MS (ESI) *m/z* calcd. for $C_{18}H_{24}N_3O^+$ $[M]^+$: 285.2; found: 285.0.

4.1.9.11. 3-(Furan-2-yl)-5-(quinuclidin-3-ylmethyl)-l,2,4-oxadiazole methiodide (31b).: CH_3I (250 μL, 4.01 mmol) was added to a solution of the free base **31** (130 mg, 0.50 mmol) in methanol. After evaporation of the solvent, the crude quaternary salt was recrystallized from methanol/absolute ethanol to give the pure compound **31b** (**31** × CH_3I). Yellowish solid; yield: 56 mg, 28%; mp 203–204 °C. ^{1}H NMR(CD_3OD, 300 MHz) δ (ppm): 7.76 (dd, *J* = 1.7, 0.6 Hz, 1H), 7.17 (dd, *J* = 3.5, 0.7 Hz, 1H), 6.65 (dd, *J* = 3.5, 1.8 Hz, 1H), 3.91–3.77 (m, 1H), 3.58–3.46 (m, 4H), 3.38–3.16 (m, 3H), 3.02 (s, 3H), 2.94–2.80 (m, 1H), 2.33–2.17 (m, 2H), 2.17–2.07 (m, 2H), 2.07–1.92 (m, 1H). ^{13}C NMR (CD_3OD, 75 MHz) δ (ppm): 179.3, 162.4, 147.0, 143.5, 115.2, 113.0, 63.0, 58.0, 57.6, 52.6, 33.6, 30.0, 25.9, 25.2, 20.2. MS (ESI) *m/z* calcd. for $C_{15}H_{20}N_3O_2^+$ $[M]^+$: 274.2; found: 274.0.

4.1.9.12. 5-(Quinuclidin-3-ylmethyl)-3-(thiophen-2-yl)-1,2,4-oxadiazole methiodide (32b).: CH_3I (742 μL, 11.9 mmol) was added to a solution of the free base **32** (410 mg, 1.49 mmol) in methanol. After evaporation of the solvent, the crude quaternary salt was recrystallized from methanol/absolute ethanol to give the pure compound **32b** (**32** × CH_3I). Yellowish solid; yield: 156 mg, 25%; mp 151–152 °C. ^{1}H NMR(CD_3OD, 300 MHz) δ (ppm): 7.82–7.76 (m,1H), 7.71 –7.65 (m, 1H), 7.24–7.16 (m, 1H), 3.91–3.76 (m, 1H), 3.51 (t, *J* = 8.1 Hz, 4H), 3.41–3.16 (m, 3H), 3.01 (s, 3H), 2.96–2.79 (m, 1H), 2.33–2.16 (m, 2H),

2.16–2.07 (m, 2H), 2.07–1.91 (m, 1H). ^{13}C NMR (CD_3OD, 75 MHz) δ (ppm): 179.3, 165.6, 130.9 (2C), 129.2, 129.1, 63.0, 58.0, 57.6, 52.7, 33.6, 30.1, 25.9, 25.2, 20.2. MS (ESI) *m/z* calcd. for $C_{15}H_{20}N_3OS^+$ $[M]^+$: 290.1; found: 290.0.

4.1.9.13. 3-Phenyl-5-(quinuclidin-3-ylmethyl)-1,2,4-oxadiazole methiodide (33b).: CH_3I (351 μL, 5.64 mmol) was added to a solution of the free base **33** (190 mg, 0.71 mmol) in methanol. After evaporation of the solvent, the crude quaternary salt was recrystallized from acetone to give the pure compound **33b** (**33** × CH_3I). Colorless solid; yield: 158 mg, 54%; mp 159–161 °C. ^{1}H NMR (CD_3OD, 300 MHz) δ (ppm): 8.09–8.03 (m, 2H), 7.58–7.47 (m, 3H), 3.93–3.80 (m, 1H), 3.58–3.47 (m, 4H), 3.40–3.18 (m, 3H), 3.02 (s, 3H), 2.99–2.83 (m, 1H), 2.34–2.17 (m, 2H), 2.17–2.07 (m, 2H), 2.07–1.93 (m, 1H). ^{13}C NMR (CD_3OD, 75 MHz) δ (ppm): 179.3, 169.5, 132.5, 130.1, 128.4, 127.9, 63.0, 58.0, 57.6, 52.7, 33.6, 30.1, 25.9, 25.2, 20.2. MS (ESI) *m/z* calcd. for $C_{17}H_{22}N_3O^+$ $[M]^+$: 284.2; found: 284.1.

4.1.9.14. 3-Methyl-5-(quinuclidin-3-ylmethyl)-1,2,4-oxadiazole methiodide (34b).: CH_3I (158 μL, 2.32 mmol) was added to a solution of the free base **34** (56 mg, 0.29 mmol) in methanol. After evaporation of the solvent, the crude quaternary salt was then recrystallized from methanol/absolute ethanol to give the pure compound **34b** (**34** × CH_3I). Reddish solid; yield: 15 mg, 15%; mp 137–138 °C. ^{1}H NMR (CD_3OD, 300 MHz) δ (ppm): 3.88–3.72 (m, 1H), 3.52 (t, J = 7.9 Hz, 4H), 3.37–3.08 (m, 3H), 3.01 (s, 3H), 2.88–2.71 (m, 1H), 2.34 (s, 3H), 2.30–2.18 (m, 1H), 2.18–2.05 (m, 3H), 2.05–1.90 (m, 1H). ^{13}C (CD_3OD, 75 MHz) δ (ppm): 178.8, 168.4, 63.0, 58.0, 57.6, 52.6, 33.6, 29.9, 25.9, 25.1, 20.2, 11.3. MS (ESI) *m/z* calcd. for $C_{12}H_{20}N_3O^+$ $[M]^+$: 222.2; found: 222.1.

4.2. Electrophysiology

Human nAChR clones obtained from Dr. Jon Lindstrom (University of Pennsylvania, Philadelphia PA) were used to heterologously express human AChRs in *Xenopus laevis* oocytes. The RIC-3 clone (human resistance-to-cholinesterase 3) was obtained from Dr. Millet Treinin (Hebrew University, Israel) and was co-injected with α7 to improve the level and speed of α7 receptor expression without affecting the pharmacological properties of the receptors [57]. Upon linearization and purification of the plasmid cDNAs, cRNAs were prepared using the mMessage mMachine in vitro RNA transcription kit (Ambion, Austin, TX). Oocytes were surgically removed from mature *Xenopus laevis* frogs (Nasco, Ft. Atkinson WI) and injected with appropriate nAChR subunit cRNAs as described previously [58]. Frogs were maintained in the Animal Care Service facility of the University of Florida, and all procedures were approved by the University of Florida Institutional Animal Care and Use Committee and have been previously described [40]. Two-electrode voltage-clamp electrophysiology experiments were conducted using OpusXpress 6000A (Molecular Devices, Union City, CA) [58]. Both the voltage and current electrodes were filled with 3 M KCl. Oocytes were voltage-clamped at −60 mV. The oocytes were bath-perfused with Ringer's solution (115 μM NaCl, 2.5 μM KCl, 1.8 μM $CaCl_2$, 10 μM HEPES, and 1 μM atropine, pH 7.2) at 2 mL/min for α7 nAChR and at 4 mL/min for α3β4 nAChR. To evaluate the effects of experimental compounds compared to ACh-evoked responses of various nAChR subtypes expressed in oocytes, control responses were defined as the

average of two initial applications of ACh made before test applications. The solutions were applied from a 96-well plate via disposable tips. Drug applications were 12 s in duration followed by a 181 s washout period for α7 nAChR and 6 s in duration followed by a 241 s washout period for α3β4 nAChR. A typical nAChR recording for each set of oocytes constituted two initial control applications of ACh, one or more experimental compound applications, and then a follow-up control application(s) of ACh. ACh controls were 60 μM for α7 and 100 μM for α3β4. The responses were calculated as both peak current amplitudes and net charge, as previously described [58]. Net-charge data are reported for α7 and peak current amplitude for all other subtypes. The averages of two initial ACh controls were used for normalization purposes for each oocyte. Data were collected at 50 Hz, filtered at 20 Hz for α7 or 5 Hz for α3β4, and analyzed by Clampfit 9.2 or 10.0 (Molecular Devices) and Excel (Microsoft, Redmond WA). Data are expressed as means ± SEM from at least four oocytes for each experiment and plotted by Excel (Microsoft, Redmond WA). Multi-cell averages were calculated for comparisons of complex responses. Averages of the normalized data were calculated for each of the 10,322 points in each of the 206.44s traces (acquired at 50 Hz), as well as the standard errors for those averages.

The new compounds were assayed for activity with the human α7 nAChR expressed in *Xenopus* oocytes using two-electrode voltage clamping as previously described [40] and compared to responses evoked by 60 μM ACh. The compound set was assayed at a concentration of 30 μM to provide a standard comparison benchmark. Based on earlier experience, this concentration is high enough to provide an observable response and low enough to avoid possible complications such as channel block. The net-charge response for each compound application is reported relative to those for ACh control applications. Data were expressed as the mean ± SEM from at least four oocytes for each experiment.

Multi-cell averages were also calculated for the display of responses in Figs. 6 and 9. The averages of normalized data were calculated using an Excel (Microsoft) template for each of the 10,500 points in each of the 210 s traces (acquired at 50 Hz). Following subtraction of the basal holding current, data from each cell, including the ACh controls, were normalized by dividing each point by the peak of the ACh control from the same cell. The normalized data were then averaged and standard errors of the mean (SEM) for the multi-cell averages calculated on a point-by-point basis. The dark lines in the plots represent the average normalized currents and the shaded areas the range of the SEM.

Supplementary Material

Refer to Web version on PubMed Central for supplementary material.

Acknowledgements

This research was financially supported by National Institutes of Health grant GM57481. The University of Milan financed the doctoral position of M.Q.

Abbreviations:

nAChR	nicotinic acetylcholine receptor

EC_{50}	half maximal effective concentration
PAM	positive allosteric modulator
PNU	PNU-120596
D_s	PAM-sensitive nonconducting desensitized state
D_i	PAM-insensitive nonconducting desensitized state

References

[1]. Papke RL, Porter Papke JK, Comparative pharmacology of rat and human α7 nAChR conducted with net charge analysis, Br. J. Pharmacol 137 (2002) 49–61. [PubMed: 12183330]

[2]. Uteshev VV, Meyer EM, Papke RL, Activation and inhibition of native neuronal alpha-bungarotoxin-sensitive nicotinic ACh receptors, Brain Res. 948 (2002) 33–46. [PubMed: 12383953]

[3]. Uteshev VV, a 7 Nicotinic ACh Receptors as a ligand-gated source of Ca^{2+} ions: the search for a Ca^{2+} optimum, Adv. Exp. Med. Biol 740 (2012) 603–638. [PubMed: 22453962]

[4]. Clark RB, Lamppu D, Libertine L, McDonough A, Kumar A, LaRosa G, Rush R, Elbaum D, Discovery of novel 2-((pyridin-3-yloxy)methyl)pipera- zines as a 7 nicotinic acetylcholine receptor modulators for the treatment of inflammatory disorders, J. Med. Chem 57 (2014) 3966–3983. [PubMed: 24814197]

[5]. Shin SS, Dixon CE, Targeting α7 nicotinic acetylcholine receptors: a future potential for neuroprotection from traumatic brain injury, Neural Regen. Res 10 (2015) 1552–1554. [PubMed: 26692836]

[6]. John D, Shelukhina I, Yanagawa Y, Deuchars J, Henderson Z, Functional alpha7 nicotinic receptors are expressed on immature granule cells of the postnatal dentate gyrus, Brain Res. 1601 (2015) 15–30. [PubMed: 25553616]

[7]. Leiser SC, Bowlby MR, Comery TA, Dunlop J, A cog in cognition: how the alpha 7 nicotinic acetylcholine receptor is geared towards improving cognitive deficits, Pharmacol. Therapeut 122 (2009) 302–311.

[8]. de Jonge WJ, Ulloa L, The alpha7 nicotinic acetylcholine receptor as a pharmacological target for inflammation, Br. J. Pharmacol 151 (2007) 915–929. [PubMed: 17502850]

[9]. Martelli D, McKinley MJ, McAllen RM, The cholinergic anti-inflammatory pathway: a critical review, Auton. Neurosci 182 (2014) 65–69. [PubMed: 24411268]

[10]. Bencherif M, Narla ST, Stachowiak MS, Alpha7 neuronal nicotinic receptor: a pluripotent target for diseases of the central nervous system, CNS Neurol. Disord. - Drug Targets 13 (2014) 836–845. [PubMed: 25012615]

[11]. Briggs CA, Anderson DJ, Brioni JD, Buccafusco JJ, Buckley MJ, Campbell JE, Decker MW, Donnelly-Roberts D, Elliott RL, Gopalakrishnan M, Holladay MW, Hui YH, Jackson WJ, Kim DJ, Marsh KC, O'Neill A, Prendergast MA, Ryther KB, Sullivan JP, Arneric SP, Functional characterization of the novel neuronal nicotinic acetylcholine receptor ligand GTS-21 in vitro and in vivo, Pharmacol. Biochem. Behav 57 (1997) 231–241. [PubMed: 9164577]

[12]. Hibbs RE, Sulzenbacher G, Shi J, Talley TT, Conrod S, Kem WR, Taylor P, Marchot P, Bourne Y, Structural determinants for interaction of partial agonists with acetylcholine binding protein and neuronal α7 nicotinic acetylcholine receptor, EMBO J. 28 (2009) 3040–3051. [PubMed: 19696737]

[13]. Robins MT, Julie Lu J, van Rijn RM, Unique behavioral and neurochemical effects induced by repeated adolescent consumption of caffeine-mixed alcohol in C57BL/6 mice, PloS One 11 (2016) 1–29.

[14]. Toyohara J, Hashimoto K, α7 nicotinic receptor agonists: potential therapeutic drugs for treatment of cognitive impairments in schizophrenia and Alzheimer's disease, Open Med. Chem. J 4 (2010) 37–56. [PubMed: 21249164]

[15]. Hauser TA, Kucinski A, Jordan KG, Gatto GJ, Wersinger SR, Hesse RA, Stachowiak EK, Stachowiak MK, Papke RL, Lippiello PM, Bencherif M, TC- 5619: an alpha7 neuronal nicotinic receptor-selective agonist that demonstrates efficacy in animal models of the positive and negative symptoms and cognitive dysfunction of schizophrenia, Biochem. Pharmacol 78 (2009) 803–812. [PubMed: 19482012]

[16]. Mazurov AA, Kombo DC, Hauser TA, Miao L, Dull G, Genus JF, Fedorov NB, Benson L, Sidach S, Xiao Y, Hammond PS, James JW, Miller CH, Yohannes D, Discovery of (2S,3R)-N-[2-(pyridin-3-ylmethyl)-1-azabicyclo[2.2.2]oct3-yl]benzo[b]furan-2-carboxamide (TC-5619), a selective α7 nicotinic acetylcholine receptor agonist, for the treatment of cognitive disorders, J. Med. Chem 55 (2012) 9793–9809. [PubMed: 23126648]

[17]. Vicens P, Ribes D, Torrente M, Domingo JL, Behavioral effects of PNU- 282987, an alpha7 nicotinic receptor agonist, in mice, Behav. Brain Res 216 (2011) 341–348. [PubMed: 20728474]

[18]. Prickaerts J, van Goethem NP, Chesworth R, Shapiro G, Boess FG, Methfessel C, Reneerkens OA, Flood DG, Hilt D, Gawryl M, Bertrand S, Bertrand D, Konig G, EVP- 6124, a novel and selective alpha7 nicotinic acetylcholine receptor partial agonist, improves memory performance by potentiating the acetylcholine response of alpha7 nicotinic acetylcholine receptors, Neuropharmacology 62 (2012) 1099–1110. [PubMed: 22085888]

[19]. Wallace TL, Callahan PM, Tehim A, Bertrand D, Tombaugh G, Wang S, Xie W, Rowe WB, Ong V, Graham E, Terry AV, Rodefer JS, Herbert B, Murray M, Porter R, Lowe SL, Lowe DA, RG3487, a novel nicotinic α7 receptor partial agonist, improves cognition and sensorimotor gating in rodents, J. Pharmacol. Exp. Therapeut 336 (2011) 242–253.

[20]. Mazurov A, Hauser T, Miller CH, Selective alpha7 nicotinic acetylcholine receptor ligands, Curr. Med. Chem 13 (2006) 1567–1584. [PubMed: 16787204]

[21]. Dallanoce C, Magrone P, Matera C, Frigerio F, Grazioso G, De Amici M, Fucile S, Piccari V, Frydenvang K, Pucci L, Gotti C, Clementi F, De Micheli C, Design, synthesis and pharmacological characterization of novel spirocyclic quinuclidinyl-D2-isoxazoline derivatives as potent and selective agonists of α7 nicotinic acetylcholine receptors, ChemMedChem 6 (2011) 889–903. [PubMed: 21365765]

[22]. Di Cesare Mannelli L, Pacini A, Matera C, Zanardelli M, Mello T, De Amici M, Dallanoce C, Ghelardini C, Involvement of α7 nAChR subtype in rat oxaliplatin-induced neuropathy: effects of selective activation, Neuropharmacology 79 (2014) 37–48. [PubMed: 24225197]

[23]. Matera C, Dondio G, Braida D, Ponzoni L, De Amici M, Sala M, Dallanoce C, In vivo and in vitro ADMET profiling and in vivo pharmacodynamic investigations of a selective α7 nicotinic acetylcholine receptor agonist with a spirocyclic D^2-isoxazoline molecular skeleton, Eur. J. Pharmacol 820 (2018) 265–273. [PubMed: 29275158]

[24]. Sarasamkan J, Scheunemann M, Apaijai N, Palee S, Parichatikanond W, Arunrungvichian K, Fischer S, Chattipakorn S, Deuther-Conrad W, Schüürmann G, Brust P, Vajragupta O, Varying chirality across nicotinic acetylcholine receptor subtypes: selective binding of quinuclidine triazole compounds, ACS Med. Chem. Lett 7 (2016) 890–895. [PubMed: 27774124]

[25]. Arunrungvichian K, Fokin VV, Vajragupta O, Taylor P, Selectivity optimization of substituted 1,2,3-triazoles as α7 nicotinic acetylcholine receptor agonists, ACS Chem. Neurosci 6 (2015) 1317–1330. [PubMed: 25932897]

[26]. Arunrungvichian K, Boonyarat C, Fokin VV, Taylor P, Vajragupta O, Cognitive improvements in a mouse model with substituted 1,2,3-triazole agonists for nicotinic acetylcholine receptors, ACS Chem. Neurosci 6 (2015) 1331–1340. [PubMed: 25978789]

[27]. Papke RL, Merging old and new perspectives on nicotinic acetylcholine receptors, Biochem. Pharmacol 89 (2014) 1–11. [PubMed: 24486571]

[28]. Kabbani N, Nordman JC, Corgiat BA, Veltri DP, Shehu A, Seymour VA, Adams DJ, Are nicotinic acetylcholine receptors coupled to G proteins? Bioessays 35 (2013) 1025–1034. [PubMed: 24185813]

[29]. Stokes C, Treinin M, Papke RL, Looking below the surface of nicotinic acetylcholine receptors, Trends Pharmacol. Sci 36 (2015) 514–523. [PubMed: 26067101]

[30]. Corradi J, Bouzat C, Understanding the bases of function and modulation of α7 nicotinic receptors: implications for drug discovery, Mol. Pharmacol 90 (2016) 288–299. [PubMed: 27190210]

[31]. Kabbani N, Nichols RA, Beyond the channel: metabotropic signaling by nicotinic receptors, Trends Pharmacol. Sci 39 (2018) 354–366. [PubMed: 29428175]

[32]. King JR, Nordman JC, Bridge SP, Lin M-K, Kabbani N, Identification and characterization of a G protein-binding cluster in α7 nicotinic acetylcholine receptors, J. Biol. Chem 290 (2015) 20060–20070. [PubMed: 26088141]

[33]. Thomsen MS, Mikkelsen JD, The α7 nicotinic acetylcholine receptor ligands methyllycaconitine, NS6740 and GTS-21 reduce lipopolysaccharide-induced TNF-a release from microglia, J. Neuroimmunol 251 (2012) 65–72. [PubMed: 22884467]

[34]. Papke RL, Bagdas D, Kulkarni AR, Gould T, AlSharari SD, Thakur GA, Damaj MI, The analgesic-like properties of the alpha7 nAChR silent agonist NS6740 is associated with non-conducting conformations of the receptor, Neuropharmacology 91 (2015) 34–42. [PubMed: 25497451]

[35]. Clark R, Lamppu D, Libertine L, McDonough A, Kumar A, LaRosa G, Rush R, Elbaum D, Discovery of novel 2-((pyridin-3-yloxy)methyl)piperazines as α7 nicotinic acetylcholine receptor modulators for the treatment of inflammatory disorders, J. Med. Chem 57 (2014) 3966–3983. [PubMed: 24814197]

[36]. Chojnacka K, Papke RL, Horenstein NA, Synthesis and evaluation of a conditionally-silent agonist for the α7 nicotinic acetylcholine receptor, Bioorg. Med. Chem. Lett 23 (2013) 4145–4149. [PubMed: 23746476]

[37]. Gronlien JH, Hakerud M, Ween H, Thorin-Hagene K, Briggs CA, Gopalakrishnan M, Malysz J, Distinct profiles of α7 nAChR positive allosteric modulation revealed by structurally diverse chemotypes, Mol. Pharmacol 72 (2007) 715–724. [PubMed: 17565004]

[38]. Briggs CA, Granlien JH, Curzon P, Timmermann DB, Ween H, Thorin-Hagene K, Kerr P, Anderson DJ, Malysz J, Dyhring T, Olsen GM, Peters D, Bunnelle WH, Gopalakrishnan M, Role of channel activation in cognitive enhancement mediated by α7 nicotinic acetylcholine receptors, Br. J. Pharmacol 158 (2009) 1486–1494. [PubMed: 19845675]

[39]. Stokes C, Israel-Assayag E, Papke RL, Program No 224.06/C24, 2013 Neuroscience Meeting Planner, Society for Neuroscience, San Diego (CA), 2013.

[40]. Papke RL, Chojnacka K, Horenstein NA, The minimal pharmacophore for silent agonism of the α7 nicotinic acetylcholine receptor, J. Pharmacol. Exp. Therapeut 350 (2014) 665–680.

[41]. Quadri M, Papke RL, Horenstein NA, Dissection of *N,N*-diethyl-*N'*-phenyl- piperazines as α7 nicotinic receptor silent agonists, Bioorg. Med. Chem 24 (2016) 286–293. [PubMed: 26707847]

[42]. Quadri M, Stokes C, Gulsevin A, Felts ACJ, Abboud KA, Papke RL, Horenstein NA, Sulfonium as a surrogate for ammonium: a new α7 nicotinic acetylcholine receptor partial agonist with desensitizing activity, J. Med. Chem 60 (2017) 7928–7934. [PubMed: 28885019]

[43]. Quadri M, Matera C, Silnovic A, Pismataro MC, Horenstein NA, Stokes C, Papke RL, Dallanoce C, Identification of α7 nicotinic acetylcholine receptor silent agonists based on the spirocyclic quinuclidine-Δ2-isoxazoline scaffold: synthesis and electrophysiological evaluation, ChemMedChem 12 (2017) 1335–1348. [PubMed: 28494140]

[44]. Papke RL, Bagdas D, Kulkarni AR, Gould T, AlSharari SD, Thakur GA, Damaj MI, The analgesic-like properties of the α7 nAChR silent agonist NS6740 is associated with non-conducting conformations of the receptor, Neuropharmacology 91 (2015) 34–42. [PubMed: 25497451]

[45]. Quadri M, Bagdas D, Toma W, Stokes C, Horenstein NA, Damaj MI, Papke RL, The antinociceptive and anti-inflammatory properties of the α7 nAChR weak partial agonist P-CF3 N,N-diethyl-N'-phenylpiperazine, J. Pharmacol. Exp. Ther 367 (2018) 203–214. [PubMed: 30111636]

[46]. Horenstein NA, Leonik FM, Papke RL, Multiple pharmacophores for the selective activation of nicotinic alpha7-type acetylcholine receptors, Mol. Pharmacol 74 (2008) 1496–1511. [PubMed: 18768388]

[47]. Bunnelle WH, Dart MJ, Schrimpf MR, Design of ligands for the nicotinic acetylcholine receptors: the quest for selectivity, Curr. Top. Med. Chem 4 (2004) 299–334. [PubMed: 14754449]

[48]. Dallanoce C, Frigerio F, Grazioso G, Matera C, Visconti GL, De Amici M, Pucci L, Pistillo F, Fucile S, Gotti C, Clementi F, De Micheli C, New spirocyclic D^2-isoxazoline derivatives related to selective agonists of α7 neuronal nicotinic acetylcholine receptors, Eur. J. Med. Chem 46 (2011) 5790–5799. [PubMed: 22014558]

[49]. Dallanoce C, Grazioso G, Pomè DY, Sciaccaluga M, Matera C, Gotti C, Fucile S, De Amici M, Investigating the hydrogen-bond acceptor site of the nicotinic pharmacophore model: a computational and experimental study using epibatidine-related molecular probes, J. Comput. Aided Mol. Des 27 (2013) 975–987. [PubMed: 24276616]

[50]. Grazioso G, Pomeè DY, Matera C, Frigerio F, Pucci L, Gotti C, Dallanoce C, De Amici M, Design of novel α7-subtype-preferring nicotinic acetylcholine receptor agonists: application of docking and MM-PBSA computational approaches, synthetic and pharmacological studies, Bioorg. Med. Chem. Lett 19 (2009) 6353–6357. [PubMed: 19804970]

[51]. Amarasinghe KKD, Maier MB, Srivastava A, Graya JL, One-pot synthesis of 1,2,4-oxadiazoles from carboxylic acid esters and amidoximes using potassium carbonate, Tetrahedron Lett. 47 (2006) 3629–3631.

[52]. Kivrak A, Zora M, A novel synthesis of 1,2,4-oxadiazoles and isoxazoles, Tetrahedron 70 (2014) 817–831.

[53]. Olesen P, Tonder J,Hansen J, Hansen H, Rimvall K, Bioisosteric replacement strategy for the synthesis of 1-azacyclic compounds with high affinity for the central nicotinic cholinergic receptors, Bioorg. Med. Chem 8 (2000) 1443–1450. [PubMed: 10896121]

[54]. Papke RL, Estimation of both the potency and efficacy of a 7 nAChR agonists from single-concentration responses, Life Sci. 78 (2006) 2812–2819. [PubMed: 16343553]

[55]. Williams DK, Wang J, Papke RL, Investigation of the molecular mechanism of the a 7 nicotinic acetylcholine receptor positive allosteric modulator PNU-120596 provides evidence for two distinct desensitized states, Mol. Pharmacol 80 (2011) 1013–1032. [PubMed: 21885620]

[56]. Papke RL, Stokes C, Damaj MI, Thakur GA, Manther K, Treinin M, Bagdas D, Kulkarni AR, Horenstein NA, Persistent activation of a 7 nicotinic ACh receptors associated with stable induction of different desensitized states, Br.J. Pharmacol 175 (2018) 1838–1854. [PubMed: 28477386]

[57]. Halevi S, Yassin L, Eshel M, Sala F, Sala S, Criado M, Treinin M, Conservation within the RIC-3 gene family. Effectors of mammalian nicotinic acetylcholine receptor expression, J. Biol. Chem 278 (2003) 34411–34417. [PubMed: 12821669]

[58]. Papke RL, Stokes C, Working with OpusXpress: methods for high volume oocyte experiments, Methods 51 (2010) 121–133. [PubMed: 20085813]

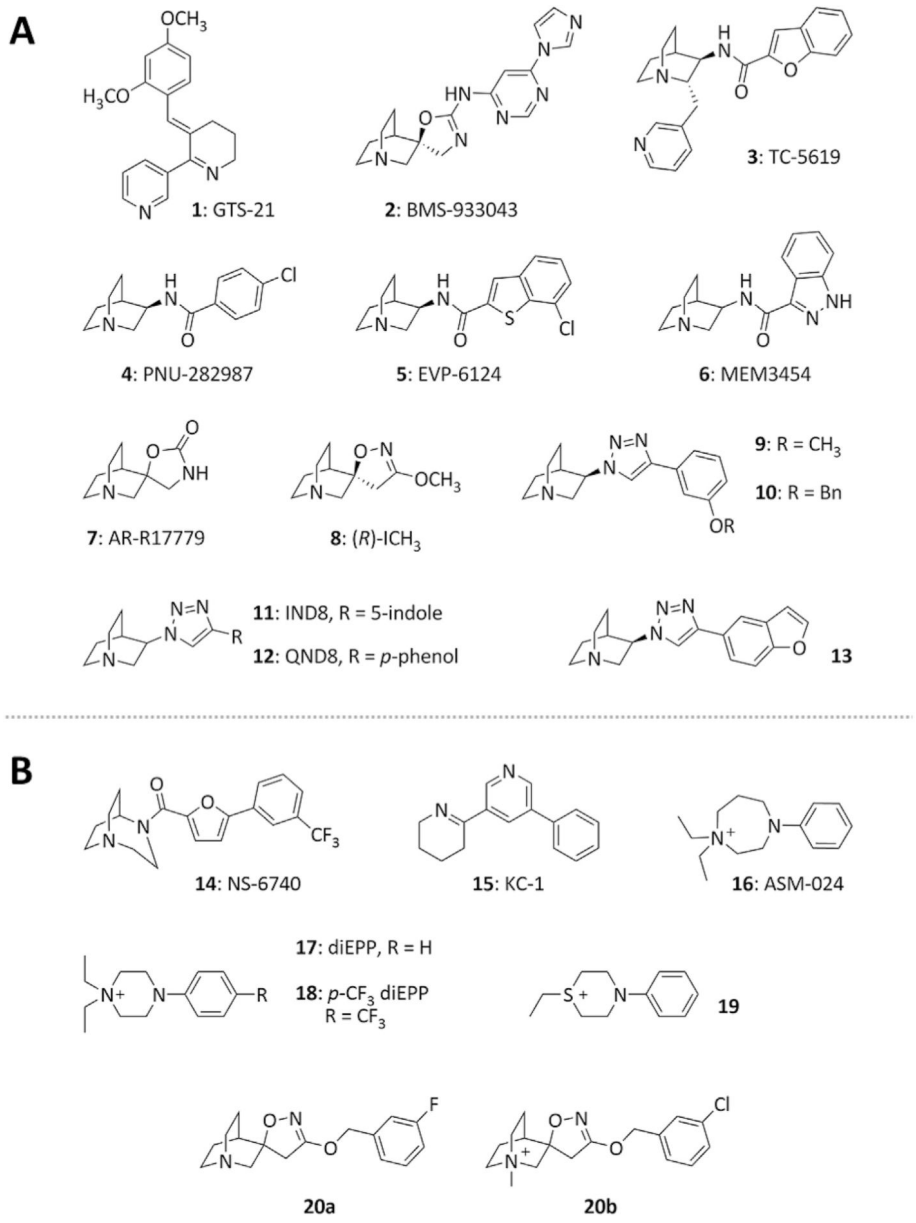

Fig. 1.

Structures of selected α7 nAChR full and partial agonists **1**–**13** (Panel A) and silent agonists **14**–**20** (Panel B).

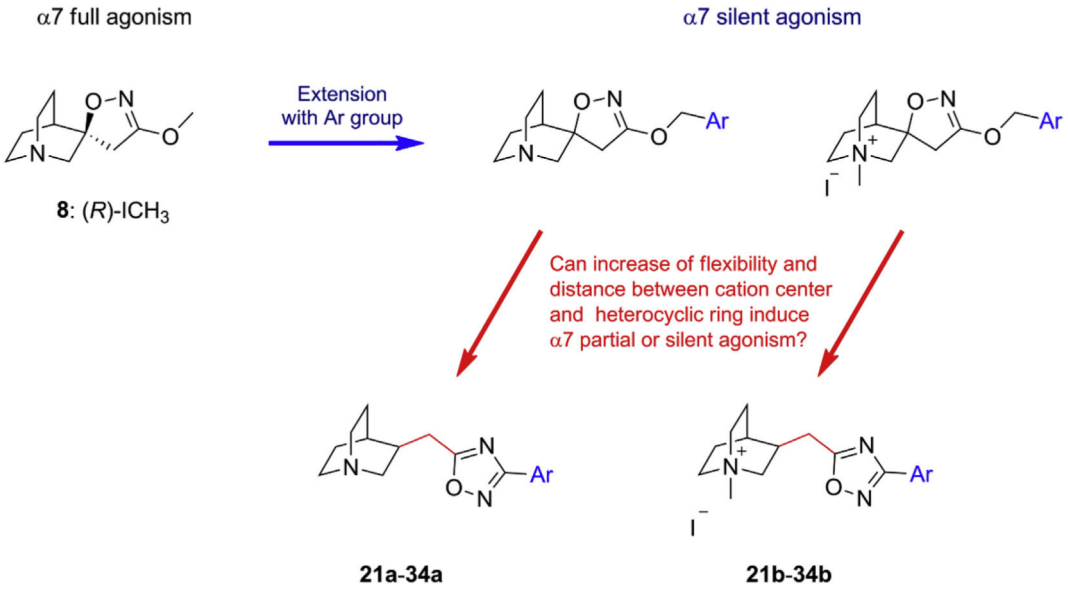

Fig. 2.

Conception of novel 5-(quinuclidin-3-ylmethyl)-1,2,4-oxadiazole derivatives **21a**-**34a** and **21b**-**34b** (for structures see Table 1).

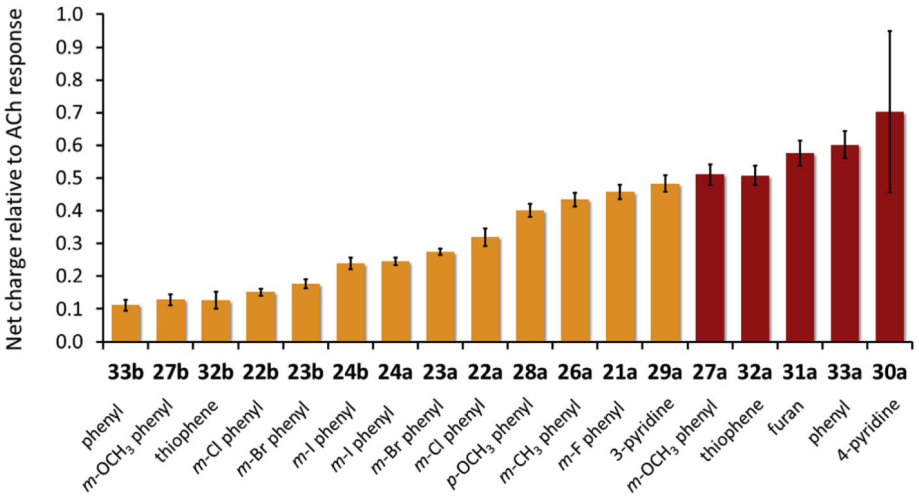

Fig. 3.

Agonist activity of the new 5-(quinudidin-3-ylmethyl)-1,2,4-oxadiazole derivatives at the α7 nAChR. Compounds of both **a** (tertiary amines) and **b** (quaternary ammonium salts) series are reported in ascending order of response magnitude. The vertical axis refers to the net-charge response evoked by compounds (30 μM), relative to ACh controls. Yellow bars represent net charge responses lower than 0.50 relative to ACh controls; red bars represent responses higher than 0.50 relative to ACh controls. Experimental values are the average of at least four independent measurements, and the error bars reflect the standard deviation of the mean. (For interpretation of the references to color in this figure legend, the reader is referred to the Web version of this article.)

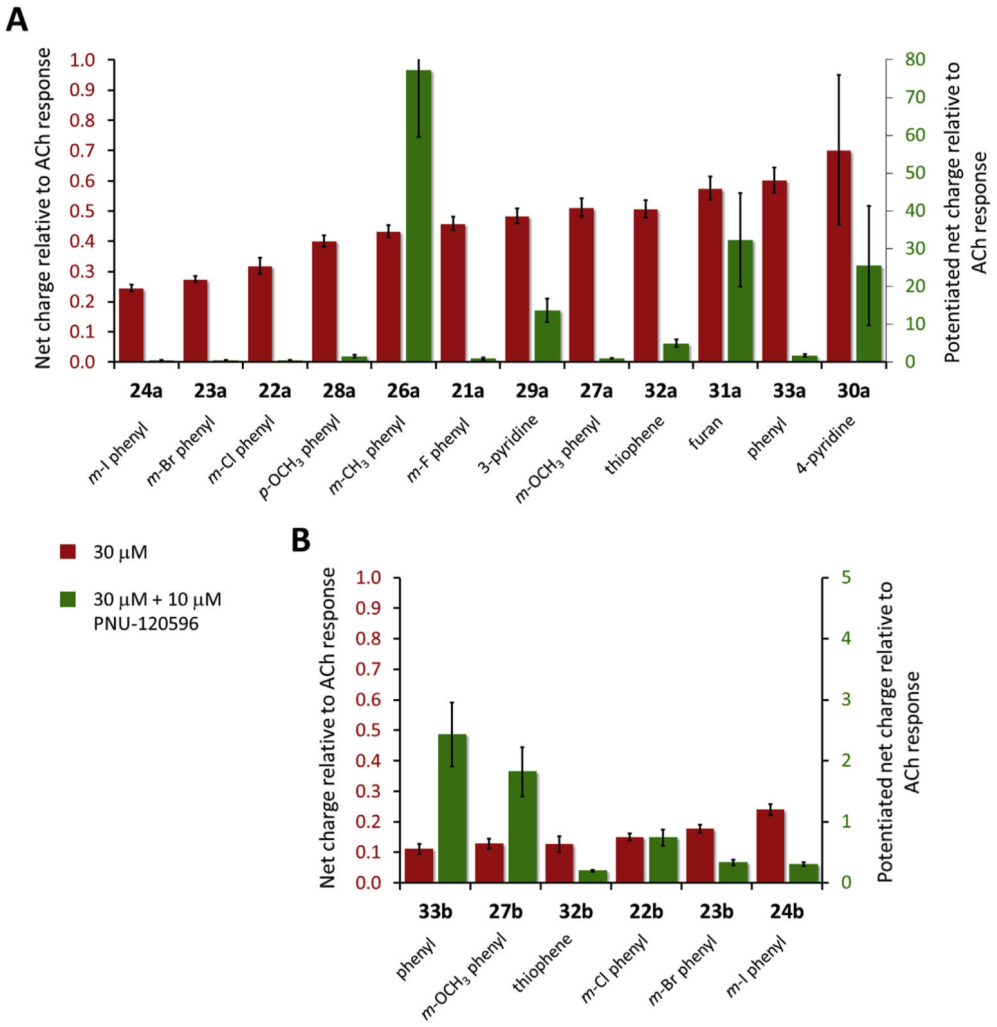

Fig. 4.

Activity of the new 5-(quinuclidin-3-ylmethyl)-1,2,4-oxadiazole tertiary amines of the **a** series (Panel A) and quaternary ammonium salts of the **b** series (Panel B) at the α7 nAChR. The vertical axis refers to the net-charge response evoked by compounds (30 μM) applied alone (red bars) or co-applied with 10 μM PNU-120596 (green bars), relative to ACh controls. Experimental values are the average of at least four independent measurements, and the error bars reflect the standard deviation of the mean. (For interpretation of the references to color in this figure legend, the reader is referred to the Web version of this article.)

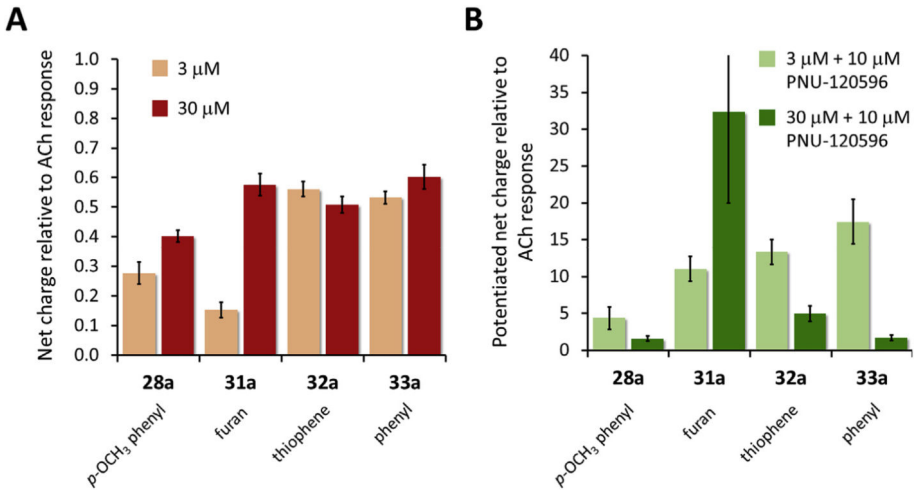

Fig. 5.

Activity of the new 5-(quinuclidin-3-ylmethyl)-1,2,4-oxadiazoles derivatives **28a**, **31a**-**33a** at the α7 nAChR. A) The vertical axis refers to the net-charge response evoked by compounds (3 and 30 μM), relative to ACh controls. B) The vertical axis refers to the net-charge response evoked by compounds (3 and 30 μM) co-applied with 10 μM PNU-120596, relative to ACh controls. Experimental values are the average of at least four independent measurements, and the error bars reflect the standard deviation of the mean.

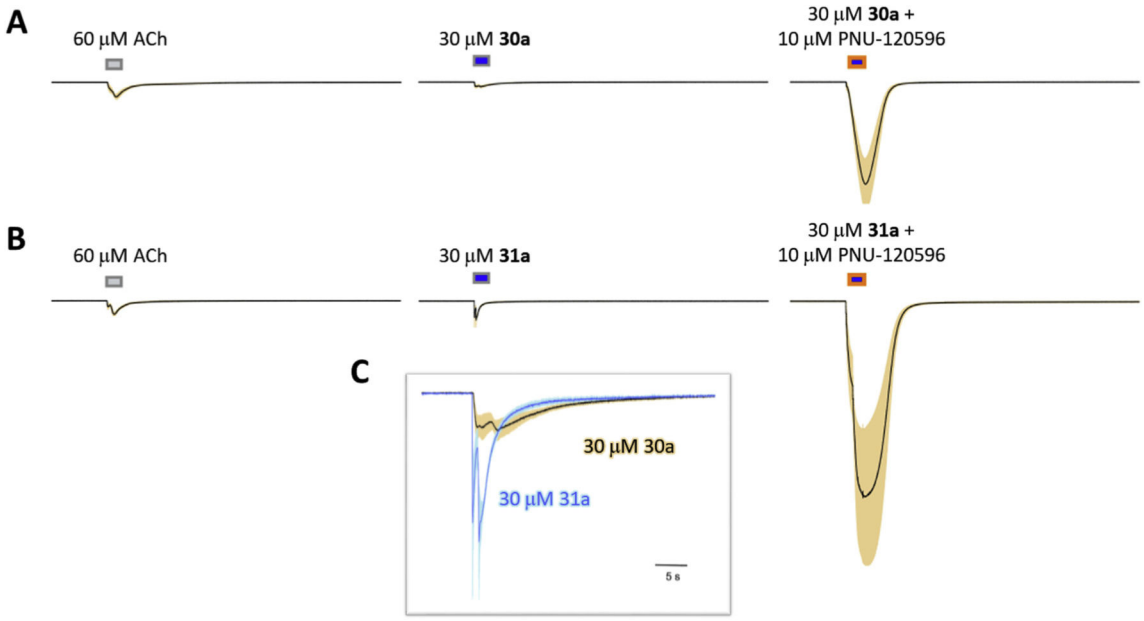

Fig. 6.

Electrophysiological responses of partial agonists **30a** and **31a**. The multi-cell averaged data traces represent the averaged normalized responses (see methods) of *Xenopus laevis* oocytes expressing human α7 nAChRs to the application of the compounds **30a** (Panel A) and **31a** (Panel B) at a probe concentration of 30 μM and in co-application with 10 μM PNU-120596, relative to averaged responses from the same cells to 60 μM ACh controls applied 4 min prior to experimental application. The ACh and drug-evoked responses were scaled in amplitude to the responses evoked in co-application with PNU-120596. The inset (Panel C) shows at a higher scale the superimposition of the traces to the application of **30a** and **31a** at 30 μM to better highlight the different partial agonist response of the two compounds.

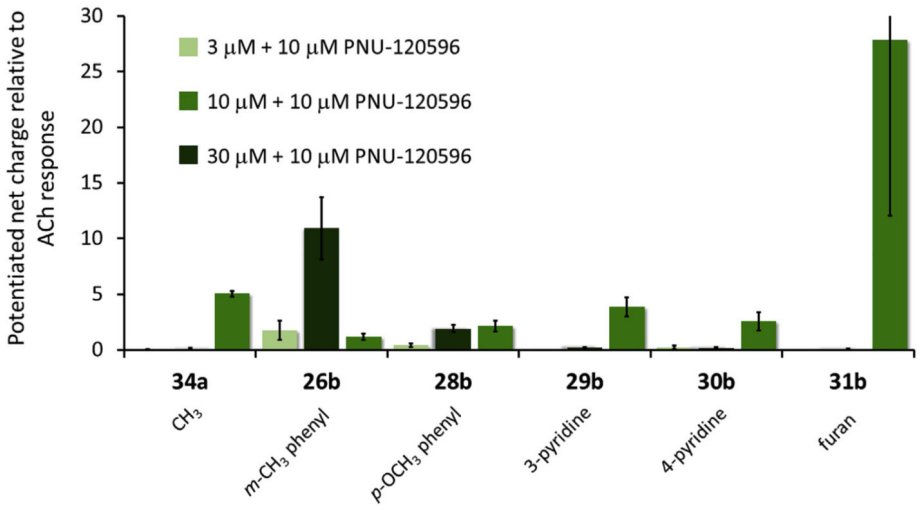

Fig. 7.

Activity of the new 5-(quinuclidin-3-ylmethyl)-1,2,4-oxadiazoles silent derivatives **34a**, **26b**, **28b**-**31b** at the α7 nAChR (**a** series: tertiary amines; **b** series: quaternary ammonium salts). The vertical axis refers to the net-charge response evoked by compounds (3 μM, 10 μM and 30 μM) co-applied with 10 μM PNU-120596, relative to ACh controls. Experimental values are the average of at least four independent measurements, and the error bars reflect the standard deviation of the mean.

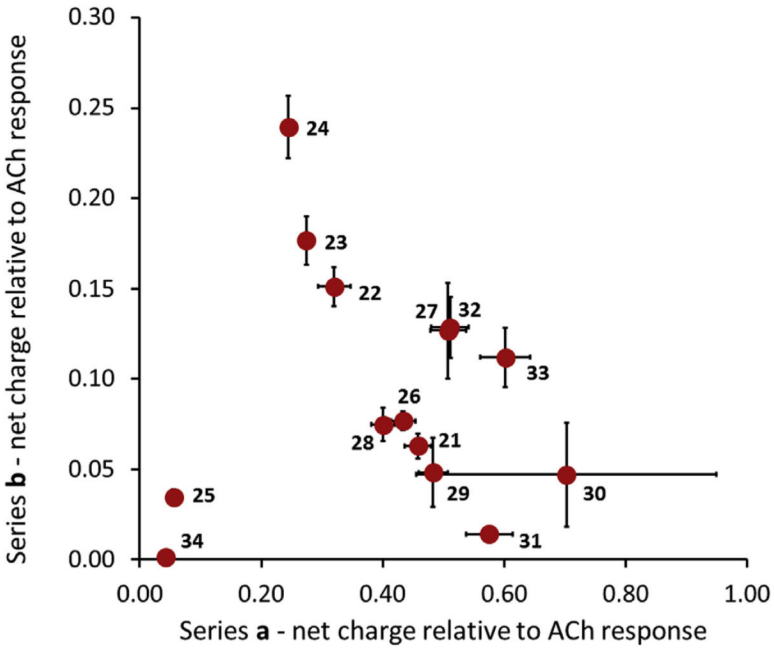

Fig. 8.

Agonist activity relationship at the α7 nAChR of compounds of the **a** and **b** series. The traces represent the averaged normalized responses (see methods) of *Xenopus laevis* oocytes expressing human nAChRs to the application of the compound **21a**-**34a** and **21b**-**34b** at a probe concentration of 30 μM. The horizontal axis represents the α7 agonist activity of tertiary amine derivatives **21a**-**34a**, expressed as net charge. The vertical axis represents the α7 agonist activity of quaternary ammonium derivatives **21b**-**34b**, expressed as net charge. Experimental values are the average of at least four independent measurements, and the error bars reflect the standard deviation of the mean.

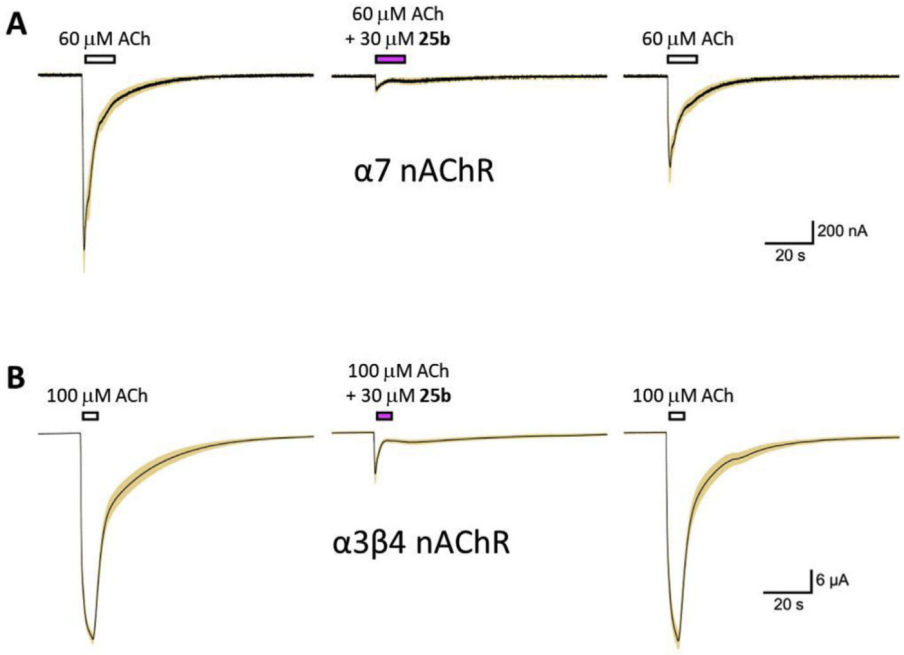

Fig. 9.

Electrophysiological antagonist responses of compound **25 b** at the α7 (Panel A) and the α3β4 nAChR (Panel B). The traces represent the averaged normalized responses (see methods) of *Xenopus laevis* oocytes expressing human nAChRs to the application of the compound **25 b** at a probe concentration of 30 μM and in co-application with 60 μM or 100 μM ACh for α7 and α3β4 nAChRs, respectively. The responses are reported as relative to averaged responses from the same cells to 60 μM and 100 μM ACh controls applied 4 min prior to experimental application. The ACh and drug-evoked responses were scaled in amplitude to the responses evoked by ACh controls.

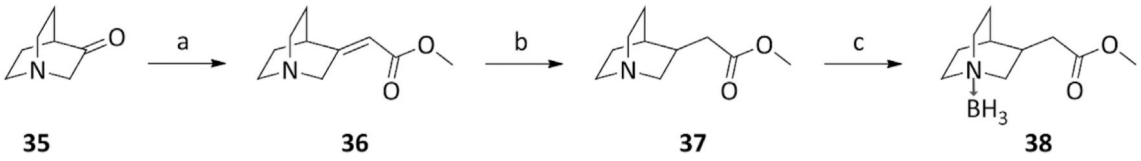

Scheme 1.

Synthetic route to key intermediate **38.** *Reagents and conditions*: a) Trimethyl phosphonoacetate (1.2 equiv), NaH (1.2 equiv), dry THF, 0 °C to rt, 1 h, then **35** (1 equiv), rt, 12 h; b) H_2, 10% Pd/C, MeOH, rt, 1 h; c) 1 M BH_3·THF complex (1 equiv), dry THF, 0 °C to rt, 1.5 h.

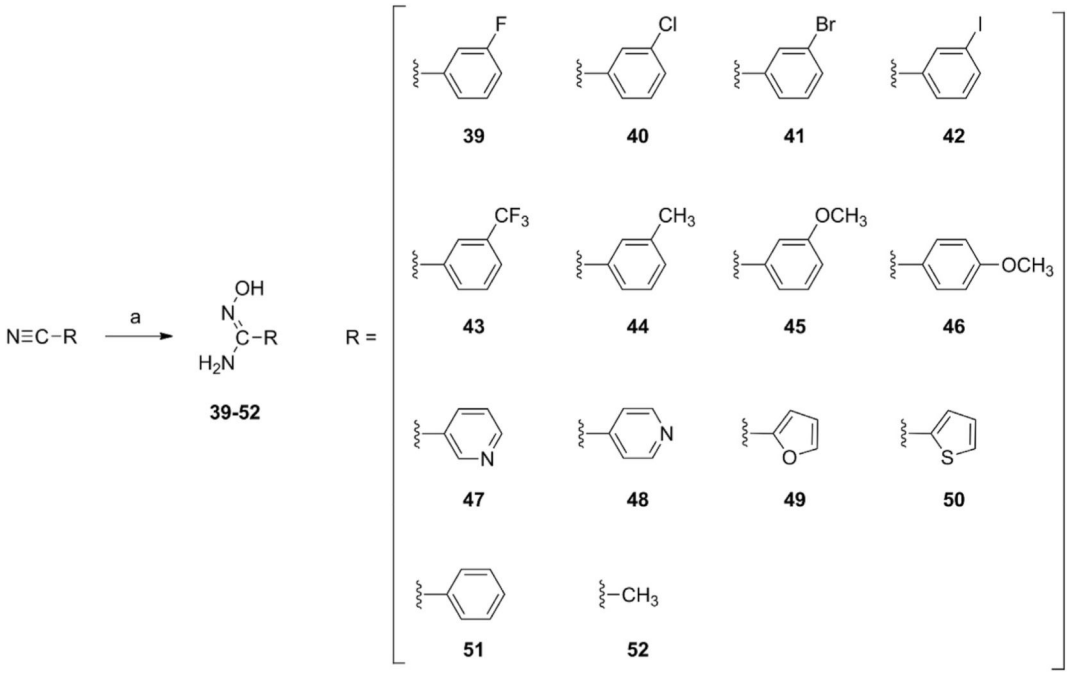

Scheme 2.

General procedure for preparation of amidoximes **39–46**,**49**, **50**, **52**. *Reagents and conditions:* a) NH_2OHH_2O (4 equiv), EtOH, 90 °C, 1 h. Amidoximes **47**,**48** and **51** are commercially available.

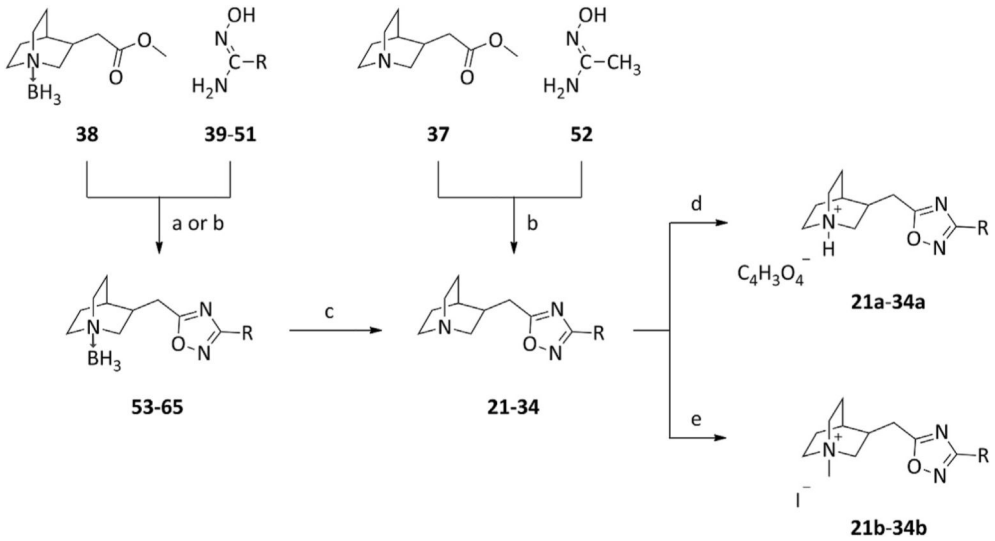

Scheme 3.

General synthetic route to 5-(quinuclidin-3-ylmethyl)-1,2,4-oxadiazoles **21a**-**34a** and **21b**-**34b**. *Reagents and conditions:* a) **39**–**52**, **44**–**46**, **49**, **51** (3 equiv), Cs_2CO_3 (3 equiv), dry THF, 50 °C, 20 min, then **38** (1 equiv.), 0 °C–80 °C, 12 h; b) **43**,**47**,**48**,**50**,**52** (3 equiv), 3 Å molecular sieves, dry THF, rt, 30 min, then NaH (3 equiv), rt to 50 °C, 20 min and then **38** (or **37** for **52**) (1 equiv.), rt to 80 °C, 12 h; c) CF_3COOH (5 equiv), acetone, 0 °C to rt, 12 h; d) fumaric acid (1 equiv), MeOH, rt, 2 h; e) CH_3I (8 equiv), MeOH, rt, 12 h.

Table 1

Structures and electrophysiological data for the partial agonist properties of derivatives **21a-34a** and **21b-34b**.

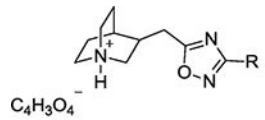

21a-34a

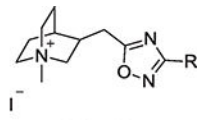

21b-34b

Compd	R	Relative response[a]			Relative response[a]		
		Peak	Net charge	Ratio	Peak	Net charge	Ratio
21	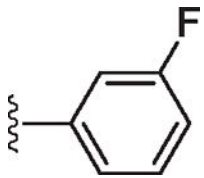	2.047 ± 0.348	0.458 ± 0.022	4.47	0.067 ± 0.012	0.063 ± 0.007	1.06
22	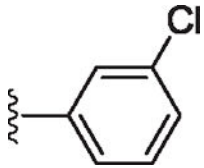	1.202 ± 0.330	0.320 ± 0.027	3.76	0.293 ± 0.046	0.151 ± 0.011	1.94
23	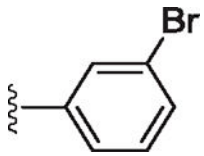	0.920 ± 0.151	0.274 ± 0.009	3.36	0.440 ± 0.070	0.177 ± 0.013	2.49
24	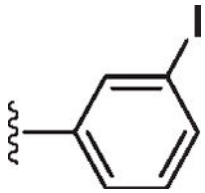	1.211 ± 0.118	0.245 ± 0.011	4.94	0.866 ± 0.251	0.239 ± 0.017	3.62

Eur J Med Chem. Author manuscript; available in PMC 2019 May 01.

Compd	R	Relative response[a]			Relative response[a]		
		Peak	Net charge	Ratio	Peak	Net charge	Ratio
25		0.144 ± 0.036	0.055 ± 0.008	2.62	0.077 ± 0.031	0.035 ± 0.004	2.20
26		2.107 ± 0.699	0.434 ± 0.020	4.85	0.079 ± 0.010	0.077 ± 0.005	1.03
27		1.415 ± 0.215	0.511 ± 0.031	2.77	0.119 ± 0.024	0.129 ± 0.017	0.92
28		1.975 ± 0.375	0.401 ± 0.020	4.93	0.051 ± 0.011	0.075 ± 0.009	0.68
29		0.867 ± 0.143	0.483 ± 0.025	1.80	0.023 ± 0.002	0.048 ± 0.019	0.48
30		0.553 ± 0.106	0.703 ± 0.247	0.79	0.034 ± 0.013	0.047 ± 0.029	0.72

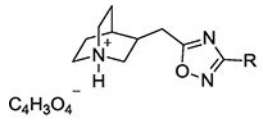

21a-34a

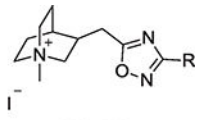

21b-34b

Compd	R	Relative response[a]			Relative response[a]		
		Peak	Net charge	Ratio	Peak	Net charge	Ratio
31	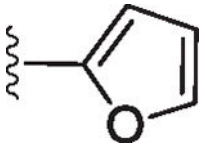	2.143 ± 0.508	0.575 ± 0.038	3.73	0.010 ± 0.002	0.014 ± 0.001	0.71
32	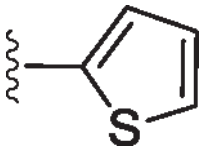	2.064 ± 0.325	0.508 ± 0.029	4.06	0.103 ± 0.012	0.127 ± 0.026	0.81
33	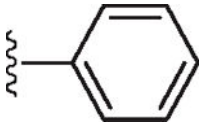	1.299 ± 0.226	0.602 ± 0.041	2.16	0.069 ± 0.015	0.112 ± 0.016	0.62
34	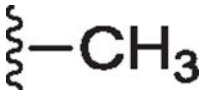	0.026 ± 0.005	0.042 ± 0.008	0.62	0.003 ± 0.001	0.001 ± 0.002	3.00

[a]"Relative response" refers to receptor response to a 30 μM application of test compound. The values are the mean ± SEM for N ≥ 4 experiments and are relative to the response of the receptor to 60 μM control applications of ACh. Details are given in the experimental section.

Table 2

Structures and electrophysiological data for the silent agonist properties of derivatives **21a-34a** and **21b-34b**.

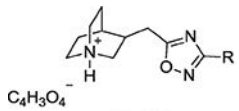

21a-34a

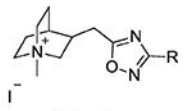

21b-34b

Compd	R	Relative response[a]	Potentiated response[a]	PNU effectiveness	Relative response[a]	Potentiated response[a]	PNU effectiveness
21	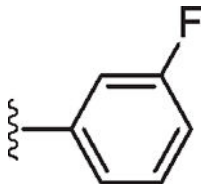	0.458 ± 0.022	0.9 ± 0.3	2	0.063 ± 0.007	0.3 ± 0.1	5
22	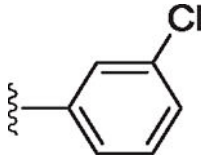	0.320 ± 0.027	0.6 ± 0.1	2	0.151 ± 0.011	0.7 ± 0.1	5
23	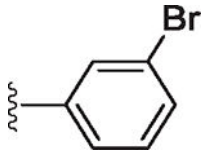	0.274 ± 0.009	0.5 ± 0.1	2	0.177 ± 0.013	0.3 ± 0.0	2
24	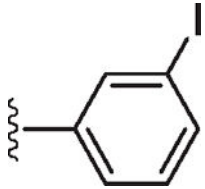	0.245 ± 0.011	0.5 ± 0.0	2	0.239 ± 0.017	0.3 ± 0.0	1

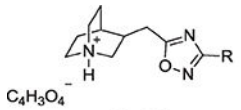

21a-34a

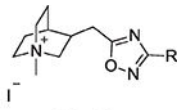

21b-34b

Compd	R	Relative response[a]	Potentiated response[a]	PNU effectiveness	Relative response[a]	Potentiated response[a]	PNU effectiveness
25	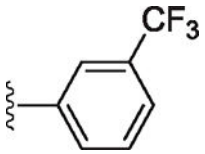	0.055 ± 0.008	0.1 ± 0.0	2	0.035 ± 0.004	0.1 ± 0.0	3
26	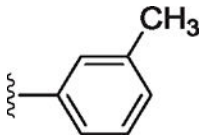	0.434 ± 0.020	77.3 ± 17.7	178	0.077 ± 0.005	1.2 ± 0.3	16
27	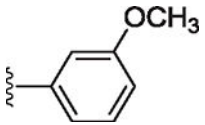	0.511 ± 0.031	1.0 ± 0.1	2	0.129 ± 0.017	1.8 ± 0.4	14
28	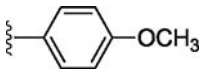	0.401 ± 0.020	1.6 ± 0.3	4	0.075 ± 0.009	2.2 ± 0.5	29
29	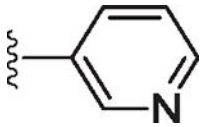	0.483 ± 0.025	13.7 ± 3.1	28	0.048 ± 0.019	3.9 ± 0.9	81
30	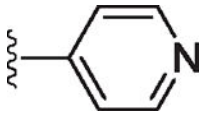	0.703 ± 0.247	25.5 ± 15.9	36	0.047 ± 0.029	2.6 ± 0.8	55

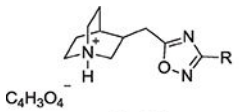

21a-34a

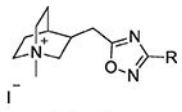

21b-34b

Compd	R	Relative response[a]	Potentiated response[a]	PNU effectiveness	Relative response[a]	Potentiated response[a]	PNU effectiveness
31	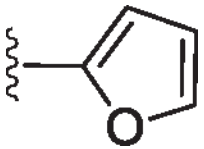	0.575 ± 0.038	32.3 ± 12.3	56	0.014 ± 0.001	27.9 ± 15.8	1993
32	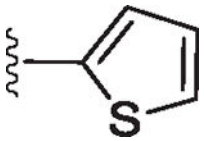	0.508 ± 0.029	5.0 ± 1.0	10	0.127 ± 0.026	0.2 ± 0.0	2
33	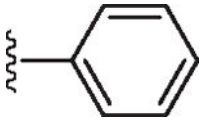	0.602 ± 0.041	1.7 ± 0.4	3	0.112 ± 0.016	2.4 ± 0.5	21
34		0.042 ± 0.008	5.1 ± 0.3	121	0.001 ± 0.002	0.1 ± 0.0	100

[a]The values are the mean ± SEM for N ≥ 4 experiments. All data are relative to the net charge response of the receptor to 60 μM control applications of ACh. “Relative response” refers to receptor response to a 30 μM application of test compound. Potentiated response refers to receptor response with 30 μM test compound and 10 μM PNU-120596 co-application. Details are given in the experimental section.